STATE OF POLAR CLIMATE

2023

CHINESE ACADEMY OF METEOROLOGICAL SCIENCES

STATE OF POLAR CLIMATE

(2023)

CHINESE ACADEMY OF METEOROLOGICAL SCIENCES

2024.06

Editorial Committee for State of Polar Climate 2023

Abstract

Polar regions are sensitive to climate change. this annual report, using various climate data, indicates that the Antarctic and Arctic showed persistent amplification effects of climate change in 2023, with frequent extreme events and notable impacts on local ecology and global weather.

The Antarctic showed slightly higher air temperature with large east-west regional differences and co-existence of extreme warm and cold events. The average annual air temperature over the Antarctica is -31.86℃, slightly higher than usual by 0.05℃. The average annual air temperature continues to rise rapidly in the Antarctic Peninsula and the West Antarctica, with three stations and seven stations recording the second and third highest autumn air temperature in history, respectively. On the contrary, the Southeast Antarctic showed cold anomalies and the Victoria Land and Wilkes Land had the coldest temperature on observation record. On July 7, the air temperature at the South Pole increased by 40℃. From mid-July to the end of August, most Antarctic experienced four extreme cold waves, with13 stations setting the lowest observed temperature record. In November, the A23a iceberg in the Weddell Sea was detached from the Antarctic ice shelf, becoming the largest iceberg in the world with area of 4,000 km^2.

Arctic warming showed a slow-down while still experienced the warmest summer post-1979 with overall distribution of "warm land-cold sea". During 1979-2023, the Arctic warming was 3.4 times the global warming rate (0.18℃/decade). Annual average air temperature of the Arctic was -9.19℃, 0.97°C higher than usual. Spring, summer, autumn and winter averaged air temperature were -12.74°C, 4.52°C, -7.09°C, and -21.14°C, respectively. Autumn and winter were obviously warmer in fall and winter. The increased air temperature reached over 2℃ in the continent around the Arctic Ocean, especially northern Canada and the Barents Sea-Kara Sea coast. Northern Canada experienced wildfires with persistence of five months with severe drought due to high temperatures anomalies and low rainfall. The peak of the Greenland ice Sheet reached 0.39°C on June 26, causing widespread melt of the ice sheet.

The rapid reduction of Antarctic sea ice continues to set new melting records, drawing global attention. On February 21, 2023, the sea ice extent(SIE) of Antarctic reached a new historical low of 1.788×10^6 km^2, surpassing the previous record in 2022. Throughout the past year, the SIE of Antarctic has consistently remained at low levels, with the annual cumulative SIE significantly below historical records. In the Arctic, the maximum SIE in 2023 was 14.62×10^6 km^2, marking the fifth lowest value on record, while the minimum SIE was 4.23×10^6 km^2, the sixth lowest on record. Due to the low sea temperatures in spring, the melting of Arctic sea ice began later than usual, however, the high temperatures in summer and autumn also delayed the refreezing process.

The Antarctic ozone hole formed earlier and lasts longer while total Arctic ozone was higher than the historical average. In 2023, the ozone hole formed about 10 days earlier, with maximum daily area of 2.6×10^7 km^2 on September 21. The Antarctic ozone hole continued to close completely until December 20, due to more Antarctic stratospheric clouds caused by the transport of material from the eruption of the Tonga volcano. Weakened Arctic polar vortex and warmer stratospheric inhibited large-scale Arctic ozone depletion, resulting in high total ozone finally. In mid-March 2024, total Arctic ozone spiked to a near-record 490 DU.

Polar atmospheric greenhouse gas concentrations show a steady upward trend, similar to the global. In 2022, annual average concentrations of carbon dioxide, methane, nitrous oxide, and sulfur hexafluoride in the Antarctic atmosphere are 414.40 ppm, 1,857.87 ppb, 334.72 ppb, and 10.78 ppt, respectively which in the Arctic atmosphere are 420.40 ppm, 1,857.87 ppb, 3,334.72 ppb, and 10.78 ppt, respectively. The average atmospheric concentrations of the main greenhouse gases in the polar regions were higher relative to them in 2022. Sulfur hexafluoride in the Antarctic and Arctic atmosphere increased by 0.38 ppt and 0.42 ppt compared to 2021, which were the largest increases of all study years.

目 录

Chapter 1 Temperature and Air Pressure

1.1 Temperature

1.1.1 Antarctic

This subsection discusses the analysis of temperature variations in Antarctica in 2023 using observational data from various Antarctic stations and first-generation global atmospheric reanalysis (CRA-40) data released by the National Meteorological Information Center. Temperature observations from the Great Wall and Zhongshan Stations are sourced from the Chinese Academy of Meteorological Sciences, while other data come from the Reference Antarctic Data for Environmental Research (Met-READER) compiled by the British Antarctic Survey, all of which have undergone quality control. In 2023, the annual average temperature of the Antarctic continent was -31.86°C, slightly higher than normal by 0.05 °C. The average temperatures for the austral summer (December to February), autumn (March to May), winter (June to August), and spring (September to November) were -21.92°C, -34.56°C, -38.85°C, and -31.77°C, respectively. In 2023, the Antarctic continent experienced colder temperatures than usual during winter and summer, with temperature decreases of 0.06°C and 0.21°C, while showing warmer anomalies during spring and autumn with temperature increases of 0.53°C and 0.15°C

The warming anomalies in 2023 were primarily observed in the Weddell Sea and its surrounding areas, continuing the pattern seen in 2022, suggesting a potential transition towards an overall warming phase in that region. Conversely, cooling anomalies were evident in the Ross Sea and neighboring regions. During the summer season, warm anomalies were most prominent around the Antarctic Peninsula and its neighboring waters. Specifically, at the Antarctic Peninsula, temperatures at the Great Wall Station and Bellingshausen Station were 0.75°C and 0.74°C higher than the long-term averages (refer to Figures 1.1-2 and 1.1-3), respectively, ranking as the second and third highest recorded temperatures. In autumn, besides the Antarctic Peninsula, notable warming was also observed in Coats Land and Queen Maud Land. Among these three regions, the stations at Mario Zucchelli, Belgrano II, and Neumayer (refer to Figures 1.1-6, 1.1-28, and 1.1-27) exhibited the strongest warm anomalies with deviations of 3.52°C, 3.44°C, and 2.66°C, respectively. Additionally, in these regions, three stations recorded the second-highest autumn temperatures (Faraday Station, Neumayer Station, Belgrano II Station, refer to Figures 1.1-8, 1.1-27, and 1.1-28), and seven stations reached the third-highest values (Orcadas Station, Changcheng Station, Bellingshausen Station, Mario Zucchelli Station, Palmer Station, Saint Martin Station, Novolazarevskaya Station, refer to Figures 1.1-1, 1.1-2, 1.1-3, 1.1-6, 1.1-7, 1.1-10, and 1.1-26). In winter, Coats Land, Queen Maud Land, and the Antarctic Peninsula persisted with warmer conditions. The Showa Station (refer to Figure 1.1-25) recorded the second-highest winter temperature anomaly at 2.65°C above average, while Belgrano II Station (refer to Figure 1.1-28) ranked third with a deviation of 2.41°C. However, in spring, the Antarctic Peninsula transitioned from warm anomalies to cooling trends, while Coats Land and Queen Maud Land maintained their warmer conditions. Neumayer Station (refer to Figure 1.1-27) recorded the second-highest spring temperature

anomaly at 3.45°C above average. On the other hand, the cooling anomalies in the Ross Sea and surrounding regions were primarily caused by cold anomalies during the winter season. Victoria Land, Princess Elizabeth Land, and Queen Mary Land experienced the most significant temperature decreases. Queen Mary Land's Marambio Station (refer to Figure 1.1-12) recorded the lowest winter temperature anomaly in history at 4.61°C below average, whereas Ross Ice Shelf Station and Zhongshan Station (refer to Figure 1.1-15 and 1.1-23) ranked as the second lowest with deviations of 3.45°C and 2.59°C, respectively. Marble Point Station (refer to Figure 1.1-14) recorded the third lowest temperature anomaly at -3.67°C below average.

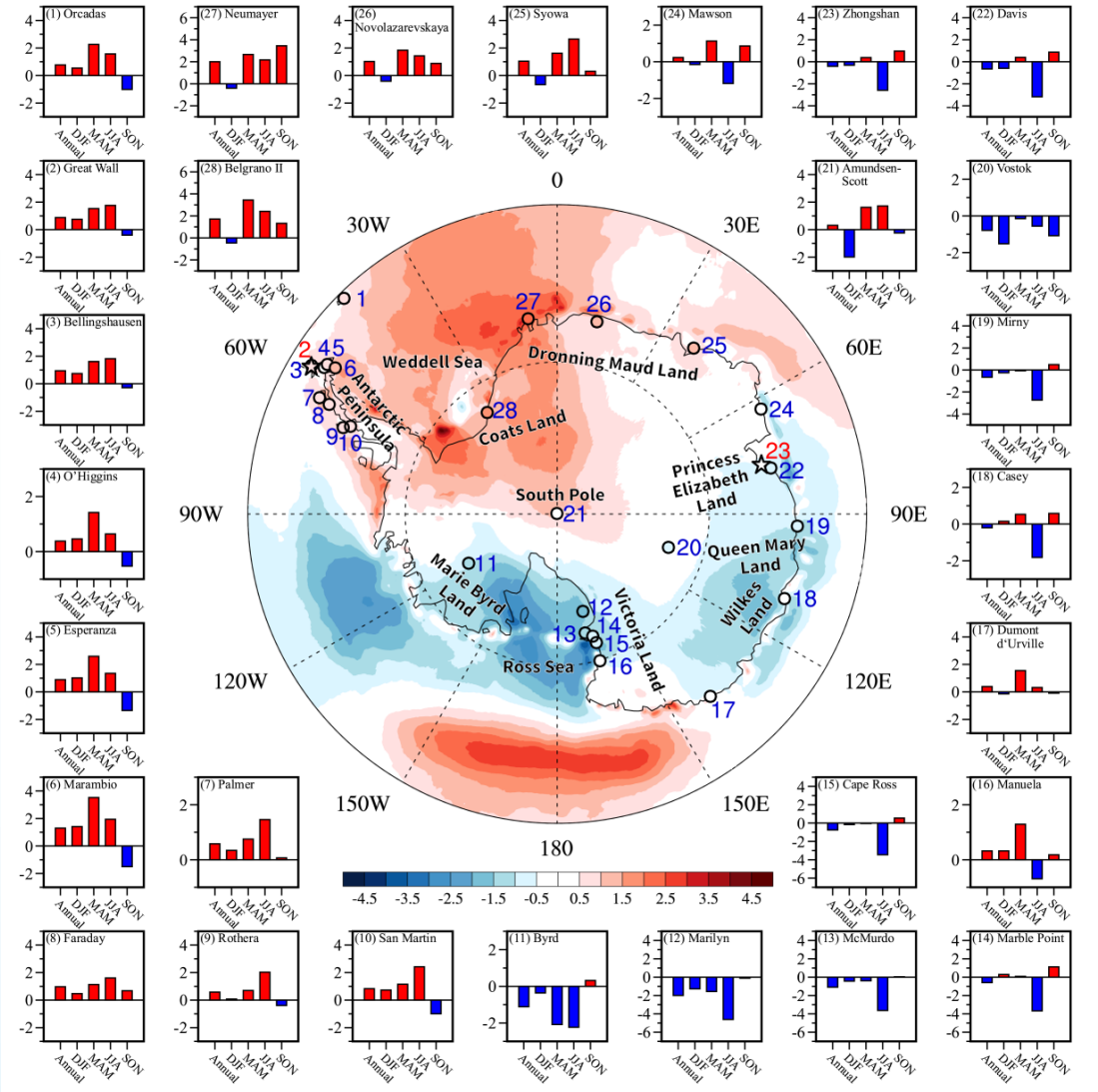

Figure 1.1 Spatial distribution of the 2023 annual mean temperature anomalies in Antarctica and the annual and seasonal mean temperature anomalies at various stations (unit: °C)

Globally, a clear upward trend in temperature is evident during the period from 1979 to 2023, with a warming rate of 0.18°C per decade (Figure 1.2). The Antarctic land temperatures exhibit a slightly higher warming rate compared to global temperatures, with a trend of 0.21°C/decade (Figure 1.2). Additionally, significant warming trends are observed in Antarctic temperatures during the austral summer, autumn, and spring, with warming rates of 0.30°C/decade, 0.17°C/decade, and 0.36°C/decade, respectively. However, the winter season shows a lower warming trend of 0.07°C/decade that does not meet statistical significance.

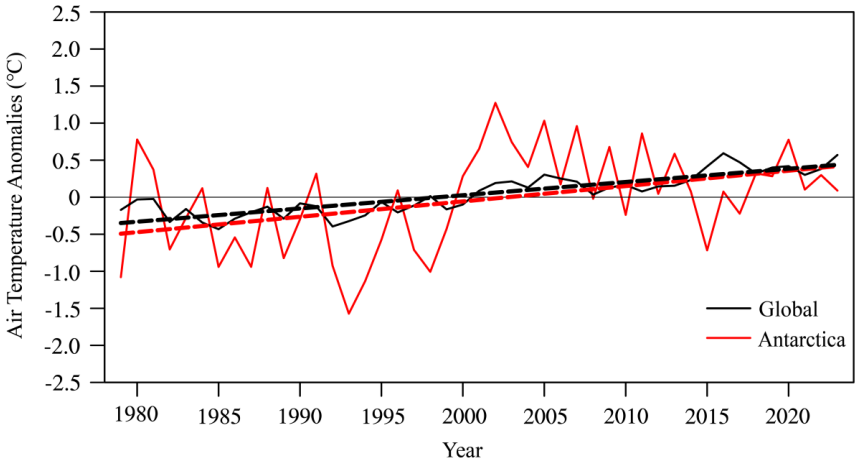

Figure 1.2 Time series of annual mean surface temperature anomalies averaged over Antarctic Continent (solid red line) and globally (solid black line) from 1979 to 2023, along with their trends (dashed lines) (unit: °C)

The trend in Antarctic land temperature changes reveals distinct regional characteristics, with certain areas displaying high sensitivity to climate change. For instance, the West Antarctic region continues

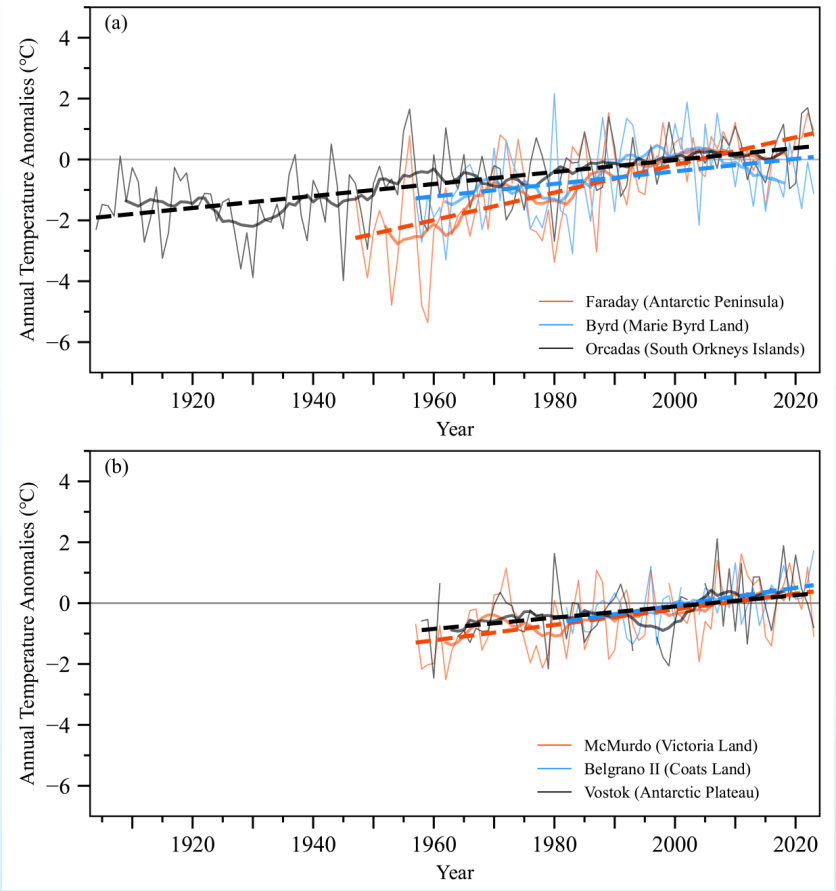

Figure 1.3 Time series of annual mean temperature anomalies at warming sites in the West Antarctic (a) and East Antarctic (b) regions. The thin solid line represents the annual mean temperature anomalies, the thick solid line represents the 11-year running average of annual mean temperature anomalies, and the dashed line indicates the trend in annual mean temperature anomalies

to experience significant warming, with the Antarctic Peninsula standing out as one of the most rapidly warming regions globally. Specifically, at Faraday Station, the annual mean temperature has been rising at a rate of 0.45°C per decade (1947-2023, depicted by the red line in Figure 1.3a). Additionally, the annual mean temperatures in the South Orkney Islands, Marie Byrd Land, Victoria Land, Coats Land, and the Antarctic Dome also exhibit a warming trend, albeit at a slower pace, with warming rates of 0.20°C per decade (1904-2023, black line in Figure 1.3a), 0.21°C per decade (1957-2023, blue line in Figure 1.3a), 0.26°C per decade (1957-2023, red line in Figure 1.3b), 0.29°C per decade (1982-2023, blue line in Figure 1.3b), and 0.18°C per decade (1958-2023, black line in Figure 1.3b), respectively. However, the annual mean temperature changes in other regions of Antarctica are less pronounced.

Extreme Events In 2023, extreme warm and cold events occurred successively in West Antarctica and East Antarctica. In July, the coldest month of the year in Antarctica, the temperature in the Antarctic Peninsula region was abnormally high. A significant extreme warm event was observed at the Amundsen-Scott Station near the South Pole. The temperature at this station soared from -74°C on July 7th to -34°C on July 8th, with a temperature increase of up to 40°C within one day. However, the average temperature at the Vostok Station on the East Antarctic continent in November set the historical lowest record since 1958, reaching -45.4°C . From mid-July to the end of August, four extreme cold events occurred in most parts of Antarctica, from eastern Antarctica to the Ross Ice Shelf, and from West Antarctica to the Antarctic Peninsula. Eleven stations set the lowest temperature observation records, causing severe delays in flights to and from Antarctica.

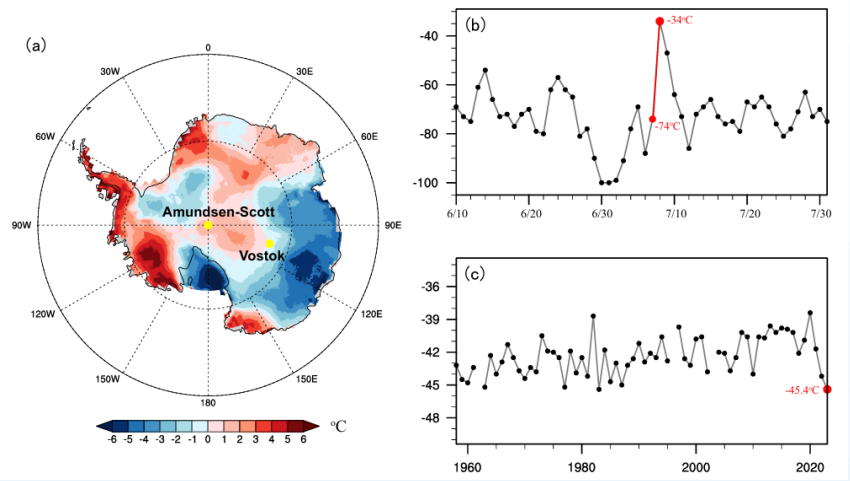

(a) The air temperature anomaly (relative to 1991–2020, based on CRA-40) in July 2023. (b) The daily series of air temperature at Amundsen-Scott station in June-July 2023. (c) The annual variation of air temperature at Vostok in November from 1958 to 2023.

On January 25, 2023, the A81 iceberg broke off from the Brunt Ice Shelf. The new iceberg has an area of approximately 1,550 km^2 and a thickness of about 150 m. In November 2023, after staying in the Weddell Sea for more than 40 years, the A23a giant iceberg left Antarctic waters for the first time and moved towards the South Atlantic. The iceberg has an area of approximately 4,000 km^2 and a thickness of more than 280 m, becoming the largest iceberg in the world at present.

1.1.2 Arctic

This subsection discusses the analysis of temperature changes in the Arctic region using data from the Global Historical Climatology Network-Daily (GHCN-D), the Greenland Weather Observations dataset from the Danish Meteorological Institute, and CRA-40 reanalysis data, all of which have undergone quality control. In 2023, the annual average temperature in the Arctic region was -9.19°C, which was 0.97°C higher than the the annual. Additionally, in 2023, temperatures in all four seasons in the Arctic region were above the long-term average. Among them, the autumn season (September to November) experienced the strongest warming with a temperature increase of 1.87°C, reaching an average temperature of -7.09°C. The winter season (December to February), spring season (March to May), and summer season (June to August) had average temperatures of -21.14°C, -12.74°C, and 4.52°C, respectively, showing deviations of 1.16°C, 0.53°C, and 0.68°C above the long-term averages.

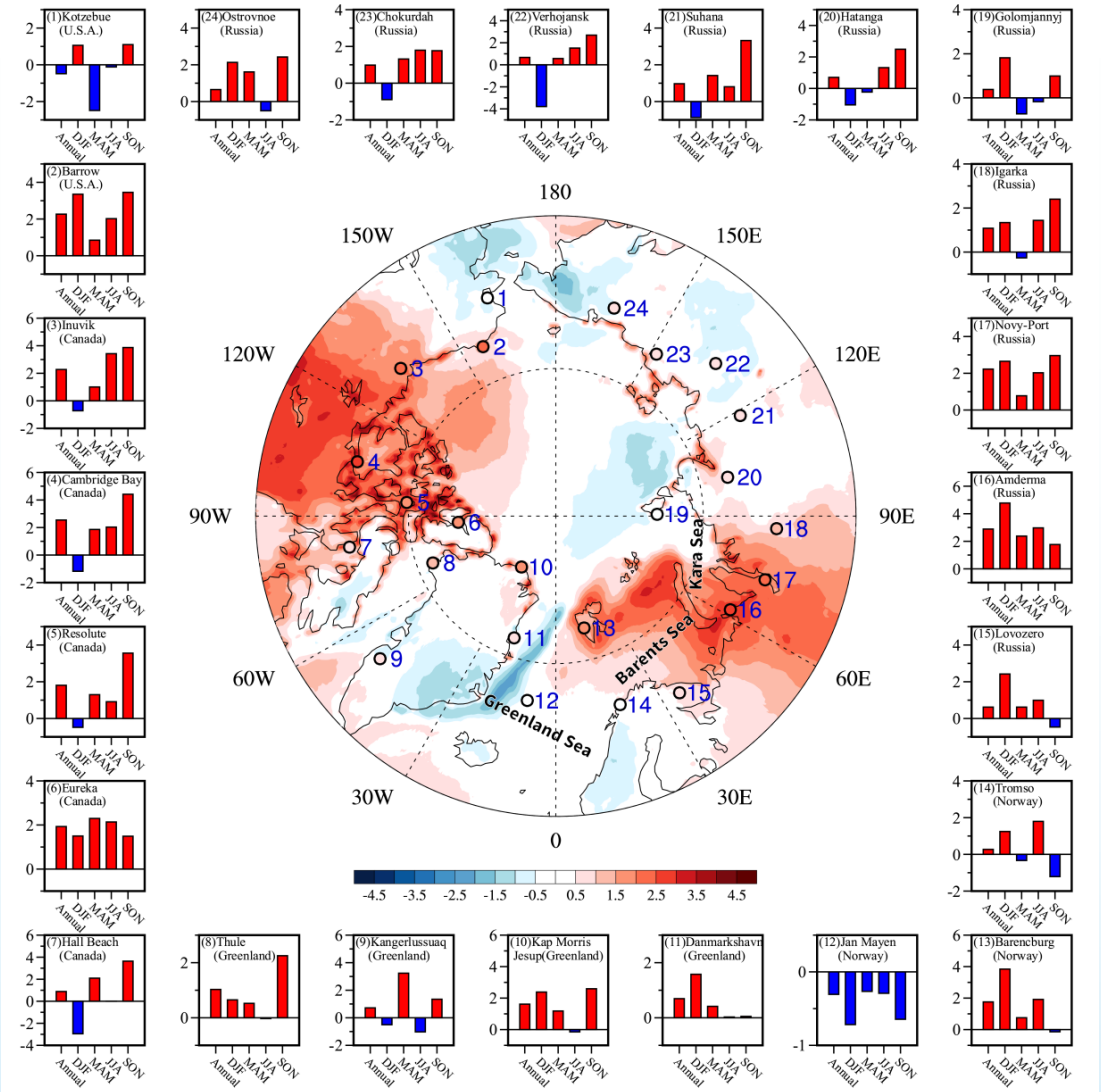

Figure 1.4 Spatial distribution of the 2023 annual mean temperature anomalies in Arctic and the annual and seasonal mean temperature anomalies at various stations (unit: °C)

In 2023, the most intense warming in the Arctic was observed along the coasts of the Barents-Kara Sea and in the Canadian Arctic region, with temperature increases exceeding 2°C. Among the stations in the Arctic region, the site with the largest temperature increase was Amarjaama, located along the coast of the Kara Sea (refer to Figure 1.4-16), with an annual average temperature of -2.4°C, which was 2.9°C higher than the long-term average, ranking as the third highest on record. Morris Jesup Point (refer to Figure 1.4-10) reached the second-highest historical annual average temperature. Poincare, Cambridge Bay, and Barrow (refer to Figure 1.4-3, 4, and 13) recorded the third-highest historical annual average temperatures. Only the Kikialik station in the United States and the Yamayan station in the Greenland Sea (refer to Figure 1.4-1 and 12) experienced cooler temperatures, with deviations of 0.5°C and 0.3°C below the long-term average. During the winter of 2023, the warming was primarily concentrated along the Barents-Kara Sea coast, with Amarjaama (refer to Figure 1.4-16) experiencing the largest temperature increase in the Arctic during winter, with temperatures 4.8°C above the long-term average. In the spring of 2023, the warm anomalies were mainly observed in the Canadian Arctic region, with Holbech (refer to Figure 1.4-7) experiencing a 2.1°C temperature increase, ranking as the third highest historical temperature. Additionally, Cambridge Bay, Eureka, and Greenland Kangerlussuaq (refer to Figure 1.4-4, 6, and 9) had temperatures 1.9 to 3.2°C above the long-term average. During the summer of 2023, the warming was concentrated along the Barents-Kara Sea coast and in the Canadian Arctic region. Poincare, Cambridge Bay, and Barrow (refer to Figure 1.4-3, 4, and 13) recorded their highest temperatures in history, while Amarjaama and Barro (refer to Figure 1.4-16 and 2) had the second-highest historical temperatures. In the fall of 2023, except for stations along the coast of the Greenland Sea experiencing cooler temperatures, all other stations exhibited warming trends. Poincare and Cambridge Bay (refer to Figure 1.4-3 and 14) recorded temperatures of 4.4°C and 3.9°C, respectively, which were the highest in history. Additionally, Holbech, Resolute, and Morris Jesup Point (refer to Figure 1.4-7, 5, and 10) had the second-highest historical fall temperatures.

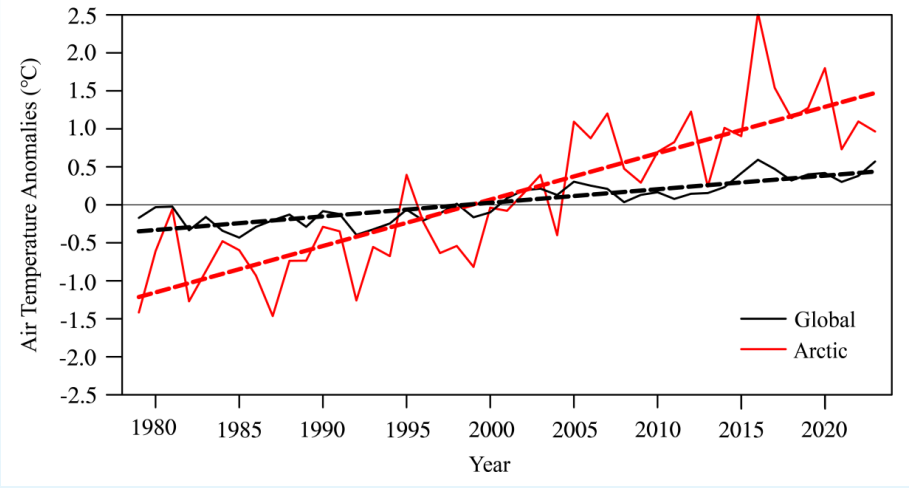

Figure 1.5 Time series of annual mean surface temperature anomalies averaged over Arctic (solid red line) and globally (solid black line) from 1979 to 2023, along with their trends (dashed lines) (unit: °C)

The annual mean temperature in the Arctic has exhibited a rapid upward trend from 1979 to 2023 (see Figure 1.5), with a warming rate of 0.61°C per decade. This rate is 3.4 times higher than the global warming rate, indicating a higher sensitivity of the Arctic to global warming. Additionally, the rapid warming in the Arctic is noticeable across different seasons, with the highest warming rates observed in autumn and winter

at 0.87°C per decade and 0.67°C per decade, respectively, while the smallest warming amplitude is recorded in summer at 0.33°C per decade.

The rapid warming in the Arctic primarily occurs over the Arctic Ocean, with slightly slower warming rates over land; nonetheless, these rates still surpass the global average warming rate. All recorded stations in the Arctic have shown a warming trend, with the warming rate accelerating further after the 1980s (refer to Figure 1.6). From 1981 to 2023, the Barrow station in Alaska experienced a warming of 1.07°C per decade, while Barrow and Amderma along the coast of the Barents-Kara Sea witnessed increases of 1.00°C and 0.90°C per decade, respectively. Conversely, locations like Daneborg, Cambridge Bay, and Vorkuta have experienced slightly slower warming rates, with temperature increases of 0.61°C, 0.58°C, and 0.52°C per decade, respectively.

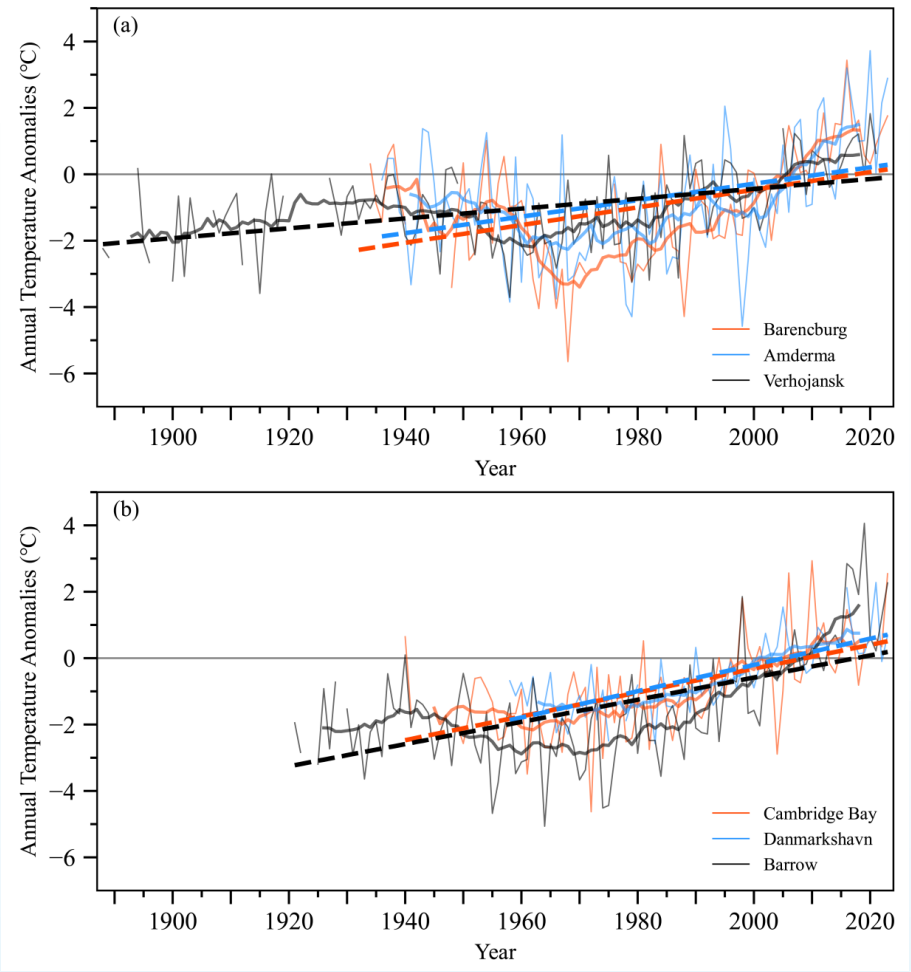

Figure 1.6 Time series of annual mean temperature anomalies at warming sites in the Arctic Eurasia (a) and North America (b) regions. The thin solid line represents the annual mean temperature anomalies, the thick solid line represents the 11-year running average of annual mean temperature anomalies, and the dashed line indicates the trend in annual mean temperature anomalies

Extreme Events In 2023, the average surface temperature of the Pan-Arctic (60–90°N) from June to August was 9.96°C, which was the hottest summer since 1979. Unusually high temperatures and low rainfall in northern Canada caused severe drought , and led to record-breaking wildfires in northwestern Canada in the summer of 2023. The wildfires lasted for more than five months, and the burned area reached 4.16 million hectares, which was the largest burned area in the 44 years on record.

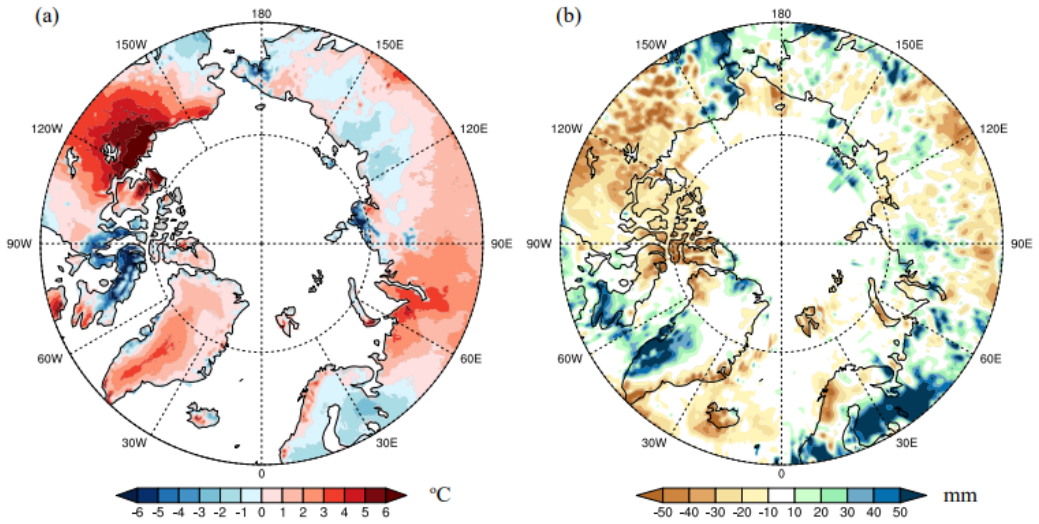

The air temperature and precipitation anomaly (relative to 1991–2020) in July 2023

The Greenland Ice Sheet experienced the warmest summer on record, with the highest point of the ice sheet reaching a temperature of 0.39°C on June 26th, which is 1.0°C above the historical record. The daily cumulative melt area of the Greenland Ice Sheet during the summer of 2023 was the second largest in the 45 years since the start of available satellite observations. On July 20, surface melting was observed across 67% of the surface of the Greenland Ice Sheet (8.44×10^5 km^2), reaching the largest single-day melt area of the year.

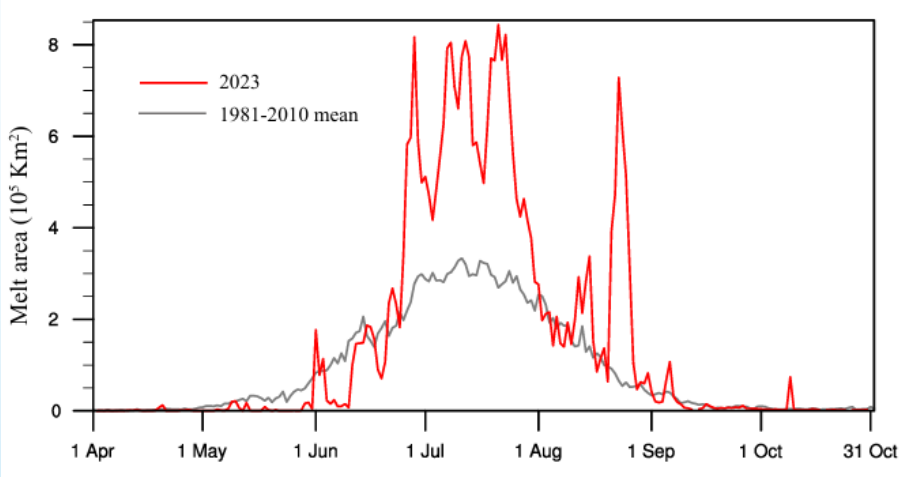

Greenland daily melts area.

1.2 Air Pressure

Air pressure is key to connecting the polar climate with the global climate. This section analyzed the characteristics of the polar pressure fields in 2023, as well as some important circulation phenomena such as the polar vortex and atmospheric oscillation. The Arctic Vortex Index is derived from the National Climate Center, while the oscillation index utilizes CRA-40 data.

1.2.1 Antarctic

The 500 hPa geopotential height fields for the austral summer (December to February of the following year, DJF) and winter (June to August, JJA) of 2023 show that the Antarctic region was dominated by large-scale low-pressure systems. During the summer, negative anomalies in the geopotential height field were observed over the Antarctic continent, while positive anomalies prevailed over the mid-latitudes. In winter, the negative anomaly area over the Antarctic continent was slightly larger than the positive anomaly area. Alternating positive and negative anomalies were observed around the Antarctic and Southern Ocean regions, indicating a pronounced zonal circulation pattern (Figure 1.7).

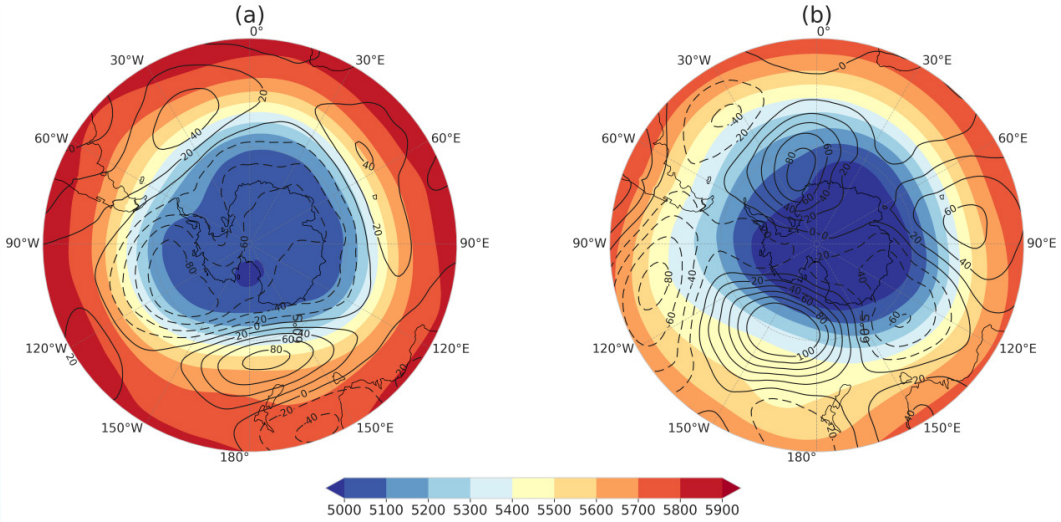

Figure 1.7 500hPa geopotential height fields (color–filled maps) and their anomalies (contour maps) for austral (a) Summer (DJF) and (b)Winter (JJA) of 2023 in Antarctica. The data are from CRA–40, with units in gpm

During 1979–2023, the Antarctic Oscillation index showed a strengthening trend（0.21/10a）, which was particularly evident in the summer (0.40/10a), with minimal variation occurring during winter. In 2023, the anomalies of the Antarctic Oscillation index in winter and summer were -1.250 and 1.922, respectively. Compared to 2022, the winter anomaly shifted from positive to negative, while the summer anomaly remained slightly stronger than normal, and the annual anomaly transitioned from a strongly positive anomaly to a moderately positive anomaly (Figure 1.8).

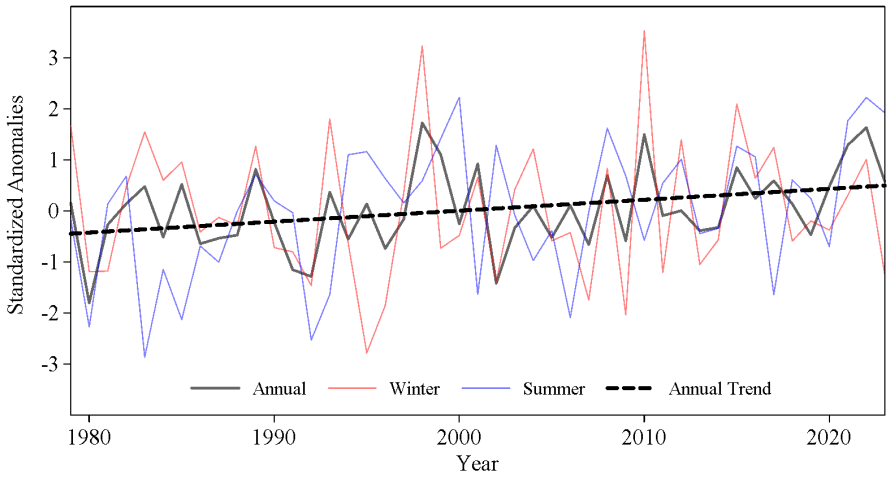

Figure 1.8 Standardized Anomalies of Antarctic Oscillation index during 1979–2023

1.2.2 Arctic

In the winter of 2023, two low-pressure centers over the Arctic appeared in the 500 hPa geopotential height field and were situated above the northern regions of East Asia and North America (Figure 1.9). Around the Arctic Circle in the winter, there was a positive anomaly in the geopotential height field, indicating a weakened Arctic polar vortex. In the summer, high-latitude regions predominantly exhibited positive anomalies in the geopotential height field.

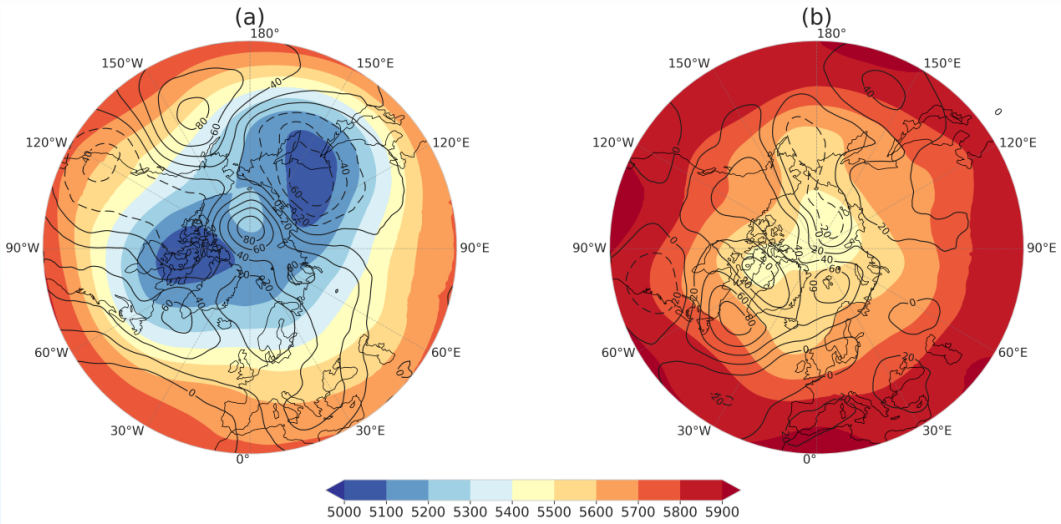

Figure 1.9 500 hPa geopotential height fields (color-filled maps) and their anomalies (contour maps) for boreal (a) winter (DJF) and (b) summer (JJA) of 2023 in Arctic. The data are from CRA-40, with units in gpm

As shown in Figure 1.10, from 1979 to 2023, there was a significant decrease in the standardized area (-0.70/10a for annual trend) and intensity (-0.61/10a for annual trend) indices of the Arctic polar vortex. In 2023, the area and intensity indices of the Arctic polar vortex exhibited notable negative anomalies during both winter and summer, indicating a weakened polar vortex.

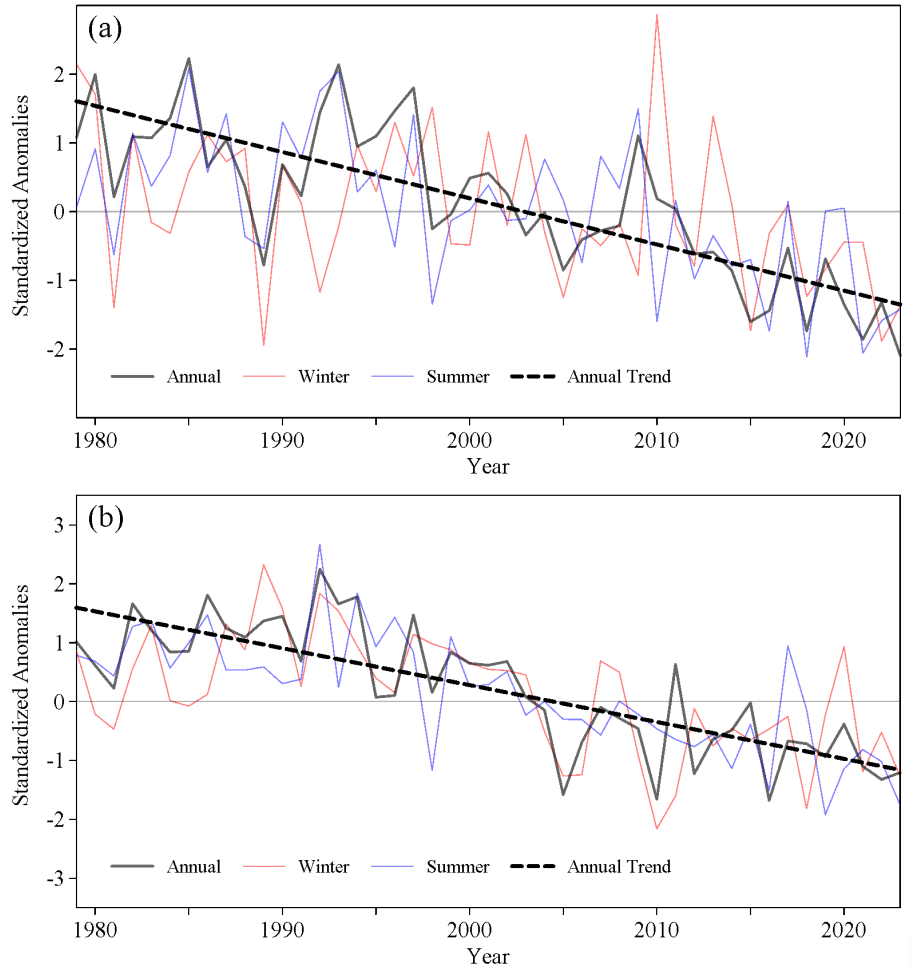

Figure 1.10 Standardized anomalies of the Northern Hemisphere polar vortex area index (a) and Northern Hemisphere polar vortex strength index (b) during1979–2023

There were no apparent trends in the Arctic Oscillation index from 1979 to 2023. The standardized anomalies of the Arctic Oscillation index for winter and summer in 2023 were 0.205 and -0.211, respectively (Figure 1.11).

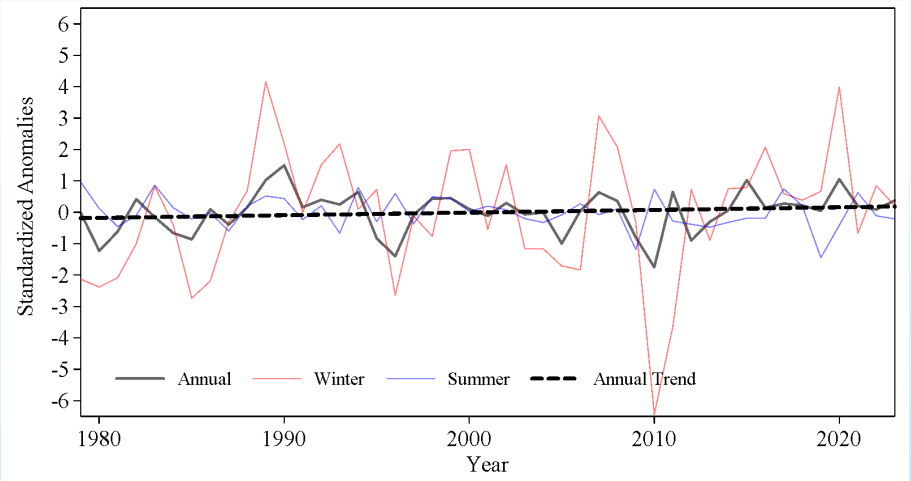

Figure 1.11 Standardized Anomalies of Arctic Oscillation index during 1979–2023

Chapter 2 Sea Ice

In this chapter, the monthly sea ice extent (SIE) from the National Snow and Ice Data Center (NSIDC) during 1979–2023 is used, with the climatology defined as the average from 1991 to 2020. In addition, sea ice concentrations from Fengyun (FY) series meteorological satellites in China(2011-2023), as well as the sea ice surface melting/freezing time dataset provided by the National Aeronautics and Space Administration of the United States (NASA) and Ocean University of China (OUC), are also used.

2.1 Sea Ice Extent

2.1.1 Antarctic

The Antarctic SIE exhibits significant seasonal variability. The freezing period typically spans from April to September, with the melting period extending from October to the following March. The minimum sea ice extent usually appears between late February and early March. Overall, the Antarctic experienced a severe anomalous low SIE throughout 2023 (Figure 2.1). Notably, the Antarctic SIE continued to remain extremely low after May 2023. Exceeding the previous two record lows on March 3, 2017 (2.11×10^6 km^2), and February 25, 2022 (1.976×10^6 km^2), a new record low was set on February 21, 2023 (1.788×10^6 km^2). Notably, the Antarctic SIE continued to remain extremely low after May 2023. Statistical analysis indicated that the SIE from January to February and from May to October 2023 were the lowest compared with those in the corresponding months over the past 45 years. The SIE in March and April 2023 was slightly greater than that in the same months in 2017, while the SIE in November was slightly greater than that in 2016, both of which were the second lowest recorded over the past 45 years. The SIE in December 2023 was slightly greater than that in 2016 and 2022, making it the third lowest value over the past 45 years. This extreme and persistent decrease in sea ice serves as a direct signal of rapid changes in Antarctic sea ice, potentially triggering further atmospheric and ecological responses.

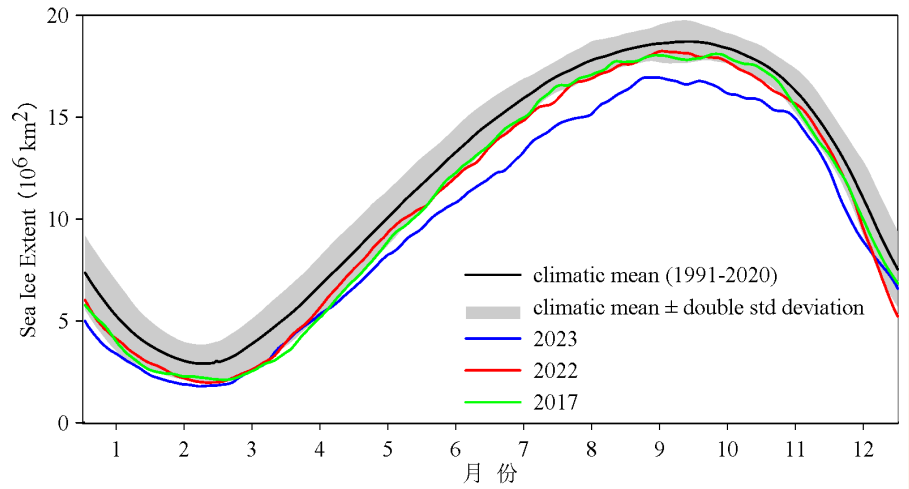

Figure 2.1 Antarctic climatic SIE, as well as the monthly Antarctic SIE in 2017, 2022, and 2023

On the interdecadal time scale, the Antarctic SIE has shown a trend of a slow increase and then a decrease between 1979 and 2023, and the declining trend has been faster in the later period. In recent years, the Antarctic SIE has set new records, with the annual minimum value reaching a new low in 2022 and again in 2023 and the annual maximum value reaching a new low for the first time in 2023 (Figure 2.2).

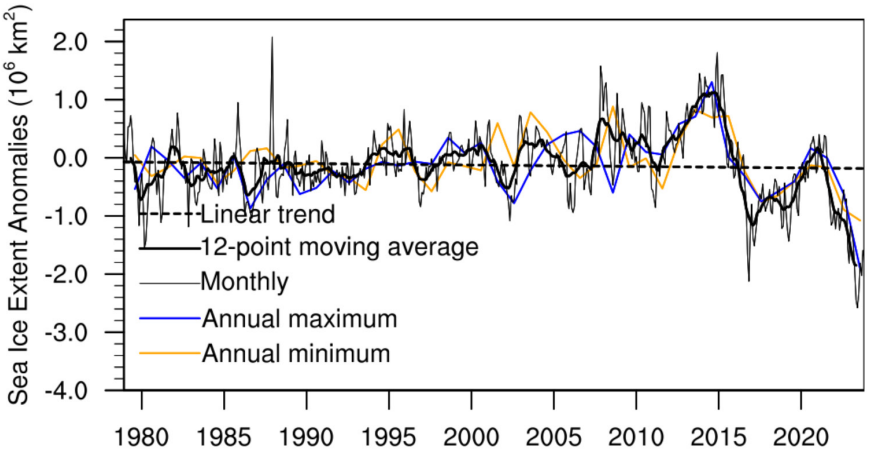

Figure 2.2 The time series of Antarctic monthly SIE anomalies and its 12-point moving average , linear trend, and the annual minimum SIE, the annual maximum SIE from 1979 to 2023

Based on the Fengyun satellite data (Figure 2.3), the Antarctic SIE in February 2023 was 2.66×10^6 km^2, which was 23.63% lower than the climatological mean (2011–2023) for the same period, setting a new low record for the Antarctic SIE at the monthly scale during the same period. In September 2023, the Antarctic SIE was 17.21×10^6 km^2, which was 8.16% smaller than the climatological mean for the same period, also setting a new low record for the Antarctic SIE at the monthly scale during the same period. From a linear trend perspective, the February SIE is decreasing by an average of 1.04×10^5 km^2 per year, while the September SIE is decreasing by an average of 1.24×10^5 km^2 per year.

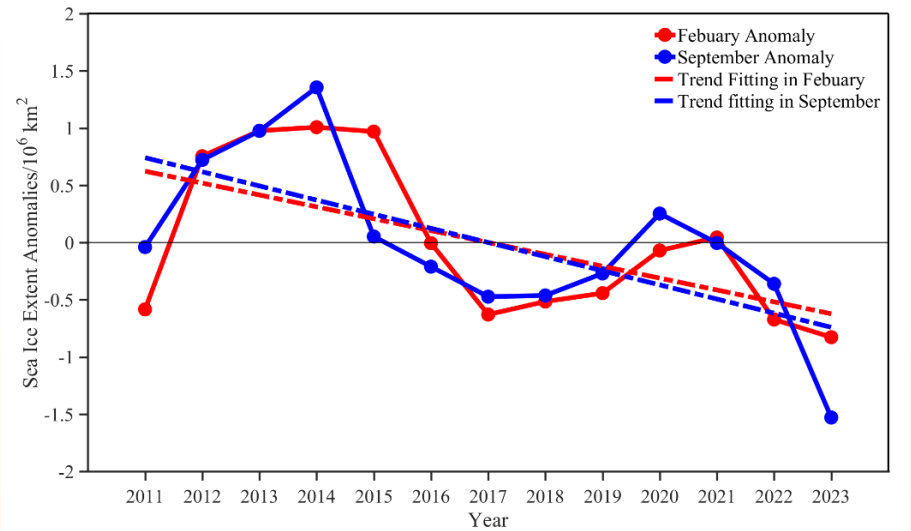

Figure 2.3 Changes in Antarctic SIE Monitored by the Fengyun Meteorological Satellites: The anomalies in February and September 2023 compared to climate mean (2011–2023)

Extreme Events The Antarctic SIE in 2023 set numerous new low records. First, the February 21, 2023, Antarctic SIE of 1.788×10^6 km^2 set a new low record for the annual minimum Antarctic SIE, while the February 2023 Antarctic SIE of 1.913×10^6 km^2 set a new low record for the monthly scale Antarctic SIE. Additionally, the September 10, 2023, Antarctic SIE of 16.956×10^6 km^2 set a new record low for the annual maximum Antarctic SIE, while the September 2023 Antarctic SIE of 16.801×10^6 km^2 was the smallest September minimum recorded in the past 45 years. In recent years, the melting rate of sea ice in the Antarctic has continued to accelerate, which has had a huge impact on the ecological environment of the Antarctic and may further affect the global weather and climate.

2.1.2 Arctic

The Arctic SIE also shows significant seasonal variability (Figure 2.4). Sea ice cover is low in the summer and autumn, reaching its annual minimum in September. In contrast, the Arctic exhibits relatively higher sea ice coverage in winter and spring, with March typically marking the annual maximum. whereas the maximum SIE of 2023 (14.62×10^6 km^2) ranked the fifth lowest in history, which was 2.01×10^6 km^2 less than the historical maximum record since remote sensing observations began in 1979, and was lower compared to the previous year. Conversely, the historical minimum of the Arctic SIE was recorded on September 17, 2012 (3.39×10^6 km^2). In 2023, the minimum extent ranked the sixth lowest, with a value of 4.23×10^6 km^2, lower than that in the previous year.

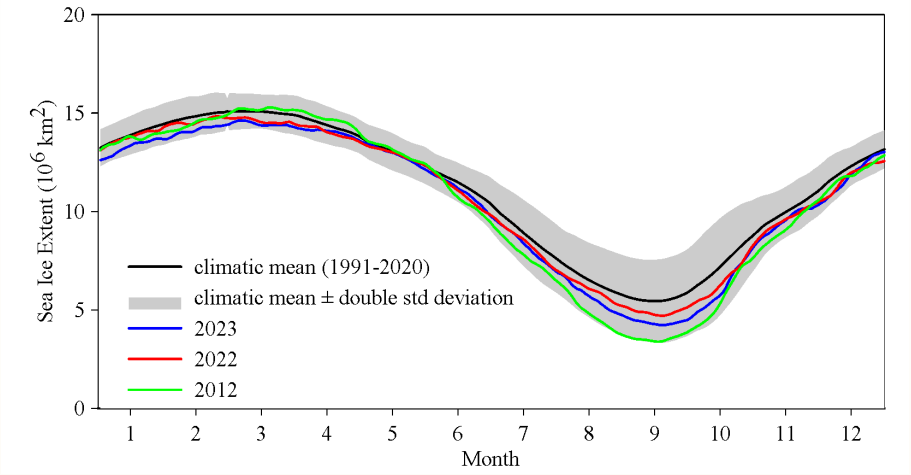

Figure 2.4 Arctic climatic SIE, as well as the monthly Antarctic SIE in 2012, 2022, and 2023

The time series of monthly Arctic SIE anomalies are shown in Figure 2.5. The Arctic SIE decreased by 0.04×10^6 km^2/decade from 1979 through 2023, and the downward linear trend in the annual minimum extent was 12.5%/decade. Notably, the decline in Arctic SIE has slowed in recent years.

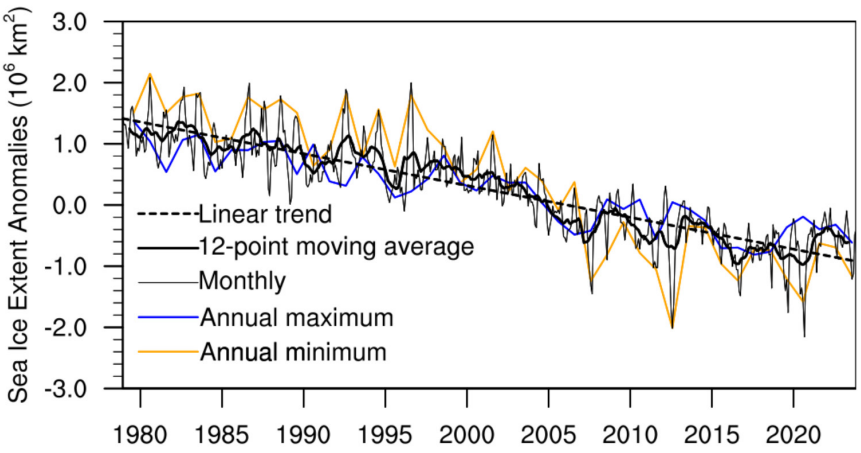

Figure 2.5 The time series of Arctic monthly SIE anomalies and its 12−point moving average , linear trend, and the annual minimum SIE, the annual maximum SIE from 1979 to 2023

Extreme Events In recent years, the persistently low SIE in the Arctic Barents and Kara Seas has contributed to a downward trend in Arctic Sea ice during the winter months. The Barents Sea SIE in 2023 reached a record minimum in late January and mid-February. Previous studies have linked this to increased heat transport from the North Atlantic Ocean, and more recent research has suggested that atmospheric rivers also contribute. Atmospheric rivers bring warmer and more humid air from the tropics and subtropics, which increases downward longwave radiation and produces rainfall that contributes to the melting of winter sea ice.

2.2 Sea Ice Concentration

2.2.1 Antarctic

Figure 2.6 shows the distributions of the monthly mean and anomaly in the Antarctic sea ice concentration in February and September 2023, respectively. In February, Antarctic sea ice was mainly distributed in the Weddell Sea, the Amundsen Sea and the Ross Sea, all of which are the main areas of perennial sea ice. Except for the sea ice concentration in the Weddell Sea, which was close to the climatological mean, the sea ice concentrations in other sea areas were abnormally low.

In September 2023, sea ice basically wraps around the Antarctic continent. The area of decreases in Antarctic sea ice was greater than the area of increases in Antarctic sea ice in September; the sea ice concentration increased in the Bellingshausen Sea, the Amundsen Sea and the western Weddell Sea and decreased in the Ross Sea. The maximum reduction in the sea ice concentration in the Ross Sea ice reached 75%. The sea ice concentration in the Indian Ocean exhibited local variations, but the variation was not significant.

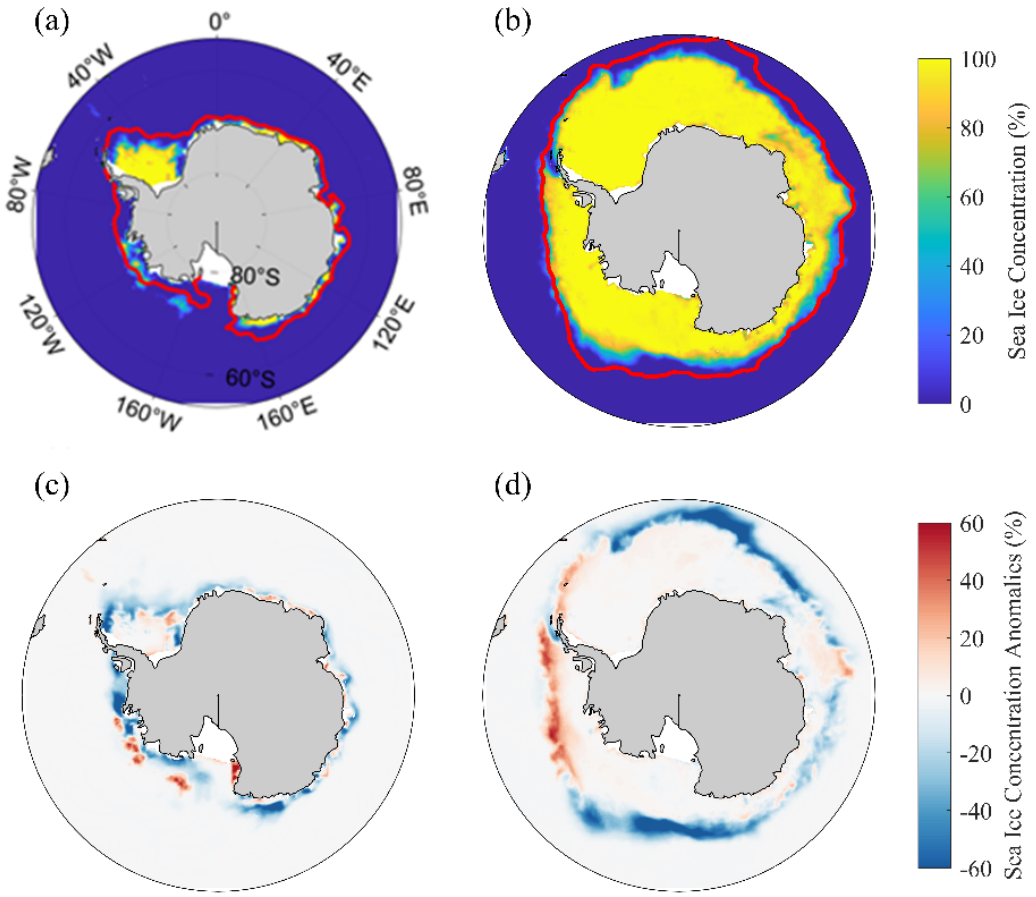

Figure 2.6 2023 Antarctic sea ice concentration and its anomaly monitored by the Fengyun meteorological satellites (unit: %) (a) monthly sea ice concentration in February 2023; (b) monthly sea ice concentration in September 2023; (c) sea ice concentration anomaly in February 2023; (d) September 2023 anomaly. The solid red line represents the average range of Antarctic sea ice from 2011 to 2023

2.2.2 Arctic

Figure 2.7 shows the monthly means and anomalies of the Arctic sea ice concentration in March and September 2023. Arctic sea ice cover has been declining for several decades, but the rate of decrease in sea ice concentration has slowed in recent years. Sea ice concentration anomalies in 2023, compared to the 2011-2023 average, were consistently negative in the ice-margin areas of the Pacific sector. The retreat of sea ice was more pronounced in September, with notable declines observed in the Canadian Archipelago, the Beaufort Sea, the Chukchi Sea, and the East Siberian Sea. In the Atlantic sector, the anomalies were negative in the Barents Sea and positive in the Greenland Sea in March. The anomalies in the ice-margin areas in September were significantly positive, particularly in the Laptev Sea.

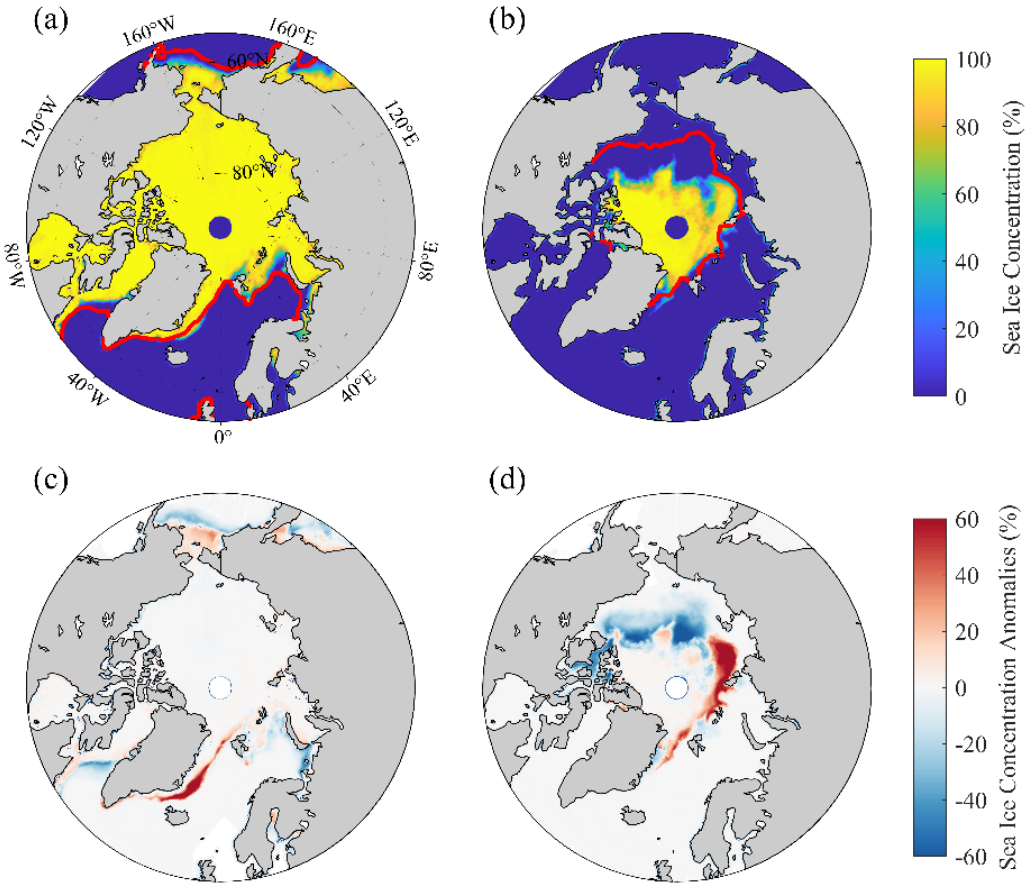

Figure 2.7 Arctic sea ice concentration and its anomalies in 2023 from FY-3 series meteorological satellites. (a) SIC on March. The red line represents the average sea ice extent for 2011–2023 (the 15% sea ice concentration boundary). (b) As in (a), but on September. (c) SIC anomaly on March. (d) As in (c), but on September

2.3 Sea Ice Melt Season Length

The onsets of melting and freezing of sea ice represent the beginning and end of the summer melt season, respectively. The melt onset (MO) refers to the continued presence of liquid water within the snow pack, and the ice surface becomes damp. The freeze onset (FO) is identified by an average surface temperature below the melting point, the growth of young ice in open water, and the refreezing of bare or lightly snow-covered ice. The period between the MO and FO is the sea ice melt season length.

The Arctic surface MO spans from late March in ice-margin areas to June in the central Arctic. Notwithstanding the advance of the Arctic sea ice surface MO, the delay of the FO, and the melt season length since 1979, the MO no longer has an advance trend during the operation of the FY-3B&D satellites.

As shown in Figure 2.8, melt in 2023 started 10 to 30 days later than the 2011-2023 average in most of the sea areas, which was closely related to the below-average temperatures in most of the Arctic Ocean from April to August. Only in the multi-year ice area in northern Canada, MO still shows an advance.

Internal variations in Arctic sea ice MO have been observed in recent decades, with the mean MO

advancing at a rate of 1.5 days per decade from 1979–2022[1] for areas north of 70°N. At the 1990s cutoff, the trend was more pronounced in the former period than in the latter (Figure 2.9). In 2023, according to observations by FY satellites, the regional mean MO north of 70°N was earlier than that in 2022 but later than that in 2020.

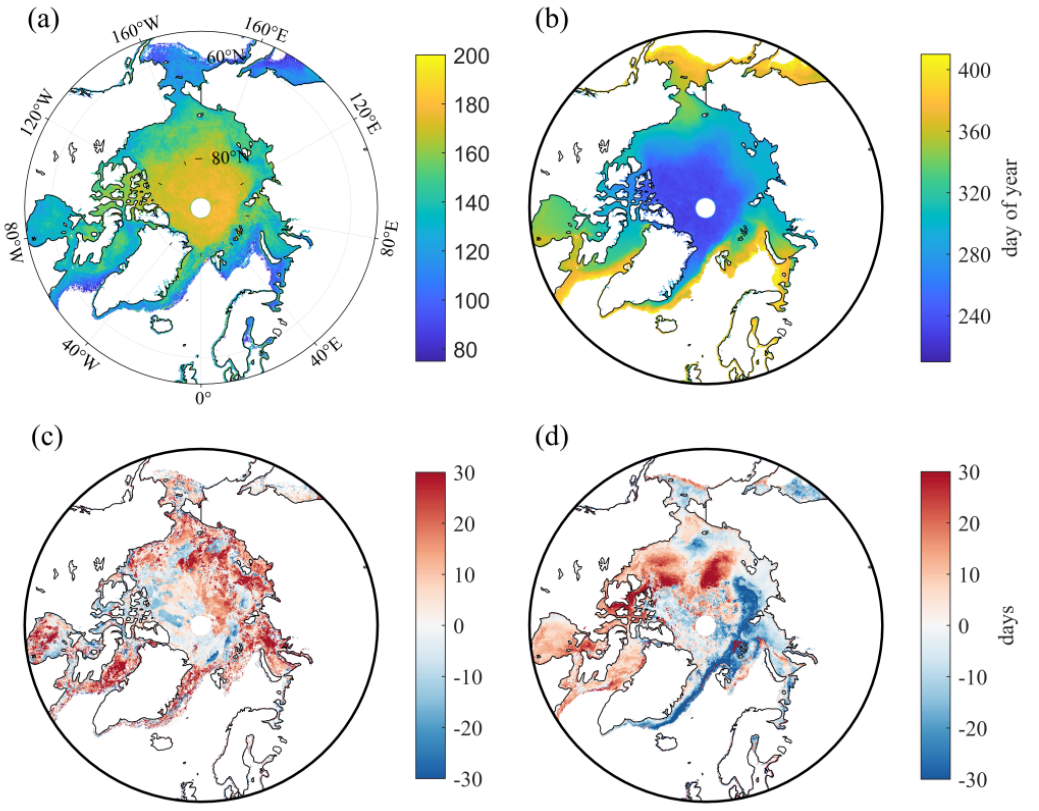

Figure 2.8 (a) Melt onset and (b) Freeze onset as averaged from 2011 to 2023. (c) Melt onset and (d) Freeze onset anomalies of 2023

The sea ice surface FO spans from August in the central Arctic to January of the following year in ice-margin areas (Figure 2.8). The FO delayed by 20-30 days in 2023 compared to the 2011-2023 average for most of the Arctic sea area, with areas of significantly delayed FOs corresponding to areas of summer sea ice retreat (Fig. 2.7d).

The mean FO trend north of 70°N since 1979 has shown a clear delay (Figure 2.9). During the operation of the FY-3B&D satellites, the inter-annual variations are obvious, manifesting as an oscillating delay trend.

The Arctic sea ice melt season length is approximately 60-90 days in the central Arctic, whereas it spans a longer period in the first-year ice areas, mainly 100-200 days, and up to more than 250 days in the ice-margin areas. From 1979 to 2022, the melt season length north of 70°N exhibited a significant trend of 6.3 days per decade (Fig. 2.9), so the continued delay of sea ice freezing in autumn dominates the trend toward a more extended melt season.

[1] Since the melt and freeze time datasets provided by NASA is currently up to 2022 and has not been updated, the time range here is 1979-2022.

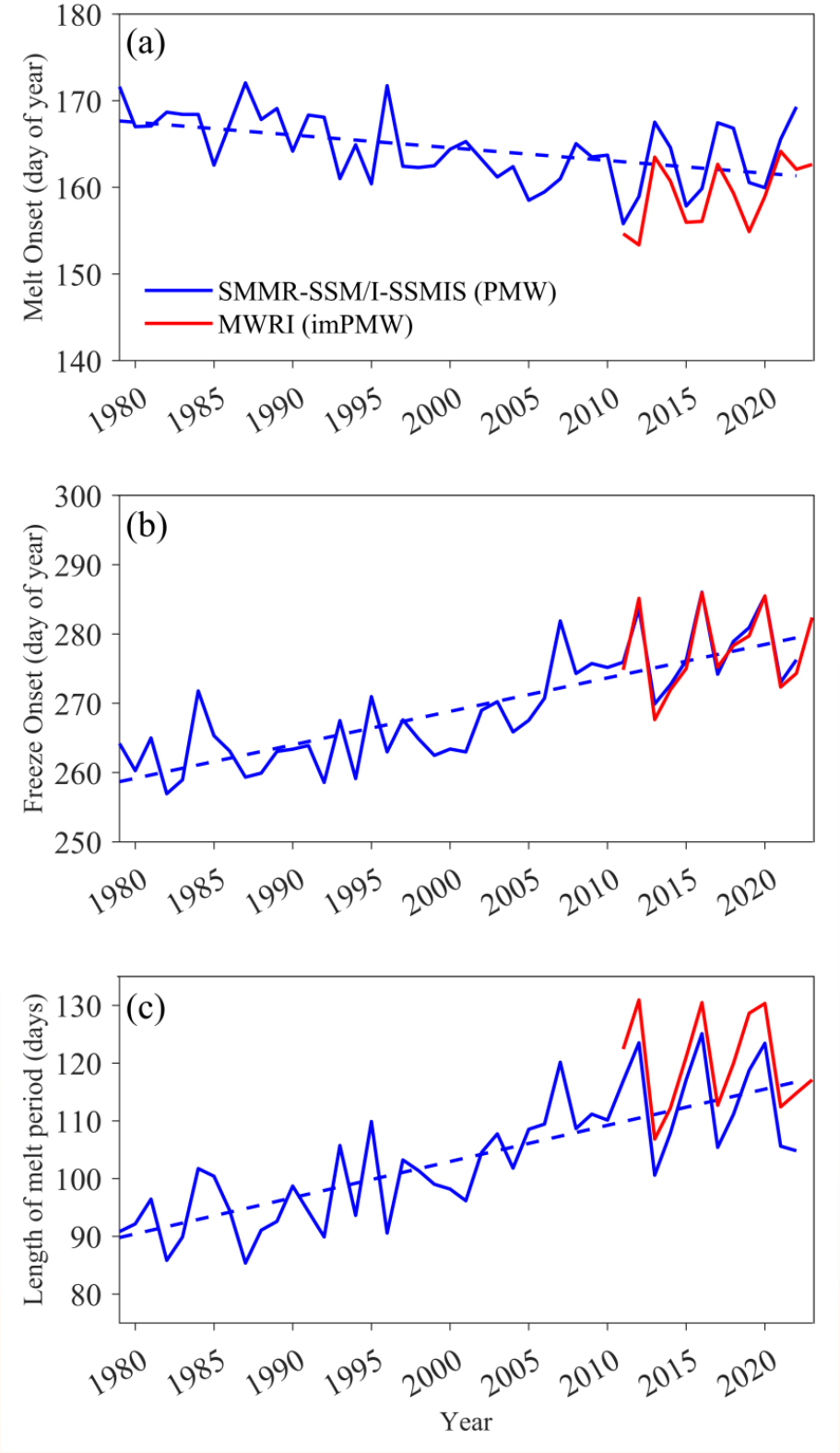

Figure 2.9 Time series of annual averages north of 70°N of (a) the melt onset, (b) the freeze onset, and (c) the length of melt season for data from NASA (blue) and OUC (red)

Chapter 3 Atmospheric Composition

3.1 Major Greenhouse Gases

This section is based on data collected at polar stations from the World Data Centre for Greenhouse Gases (WDCGG) and China's Zhongshan Station. There are 11 stations in Antarctica and 15 stations in the Arctic (Figure 3.1), covering the period from 1984 to 2022 (the concentrations of these greenhouse gases have currently only been published up to 2022). This section mainly focuses on the changes in four major greenhouse gases, i.e., CO_2, CH_4, N_2O, and SF_6.

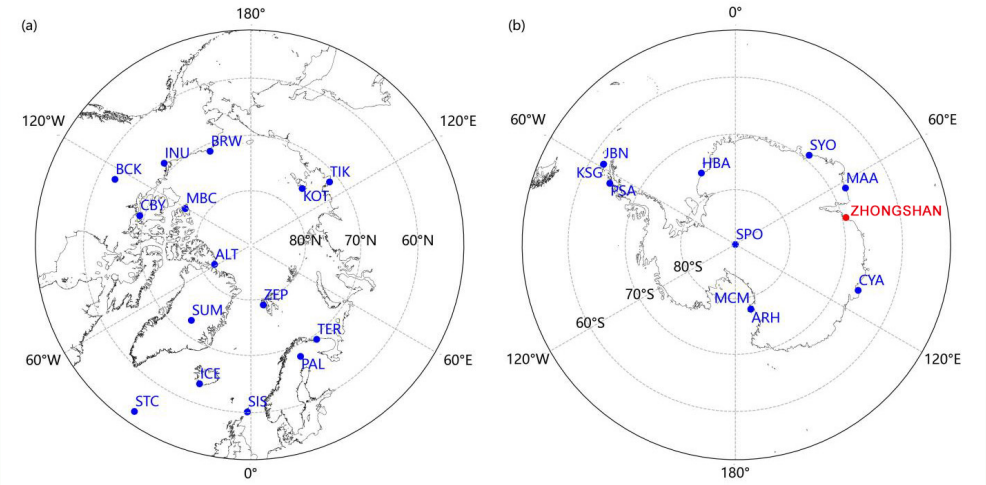

Figure 3.1 Locations of major polar atmospheric composition observation stations

3.1.1 Antarctica

(1) CO_2 and CH_4

From 1984 to 2022, the concentration of CO_2 in the Antarctic atmosphere steadily increased annually, with a growth rate of 1.87 ppm/year, which was consistent with the global trend. However, the average concentration was 2.48 ppm lower than the global average (Figure 3.2a). In 2022, the annual average concentration of CO_2 in the Antarctic atmosphere reached 414.40 ppm, an increase of 2.38 ppm compared to that in 2021. The annual average concentration of CO_2 at Zhongshan Station in 2022 was 413.84 ppm, an increase of 2.24 ppm compared to that in 2021.

Similarly, from 1984 to 2022, the CH_4 concentration in the Antarctic atmosphere also exhibited a steady year-on-year increase, with a growth rate of 5.42 ppb/year. This trend was consistent with the global trend, but the average concentration was 61.07 ppb lower than the global average (Figure 3.2b). In 2022, the annual average concentration of CH_4 in the Antarctic atmosphere reached 1857.87 ppb, an increase of 18.58 ppb compared to that in 2021. The annual average concentration of CH_4 at Zhongshan Station in 2022 was 1856.96 ppb, an increase of 18.34 ppb compared to that 2021.

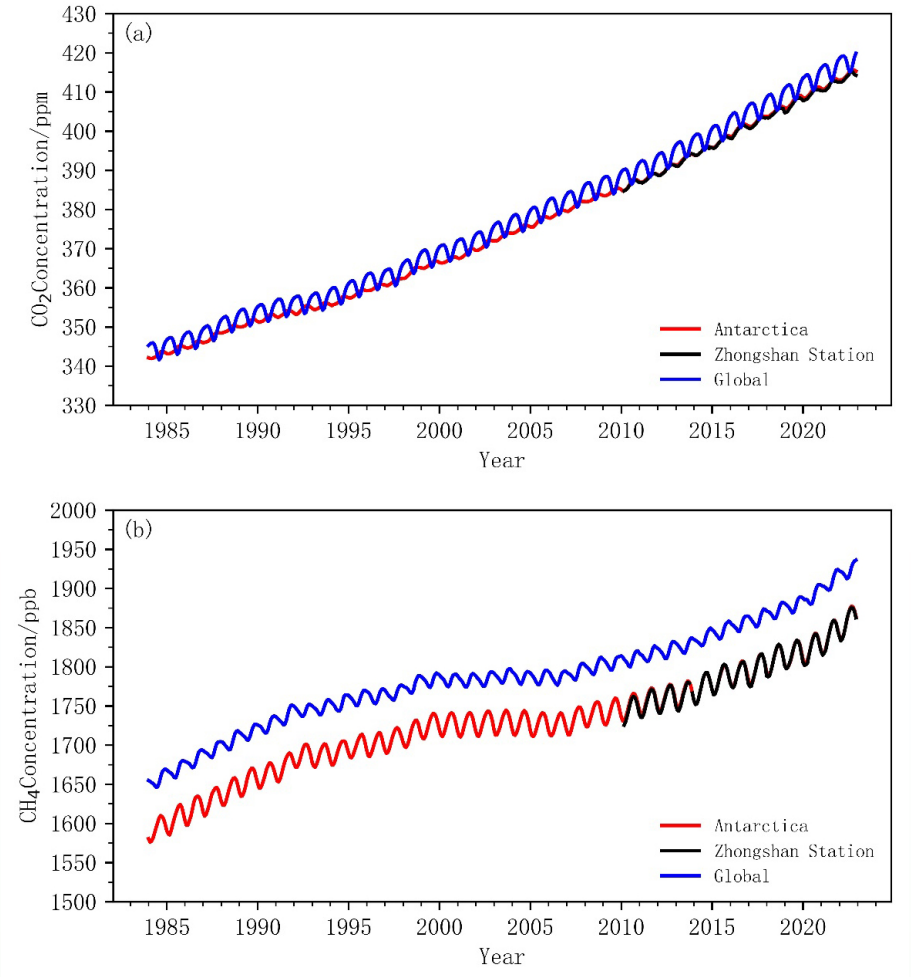

Figure 3.2 Changes in concentrations of CO2 (a) and CH4 (b) in Antarctica and the globe, 1984 to 2022

(2) N_2O and SF_6

Currently, N_2O is monitored at seven Antarctic stations. The annual average concentration of N_2O increased from 312.05 ppb in 1997 to 334.72 ppb in 2021, with annual growth rates ranging from 0.40 ppb/year to 1.54 ppb/year and an average growth rate of approximately 0.91 ppb/year (Figure 3.3a). In 2022, the annual average concentration of N_2O in Antarctica increased by 1.4 ppb compared to that in 2021. At China's Zhongshan Station, N_2O monitoring began in 2008, and the overall trend was consistent with that of the Antarctic average. From 2008 to 2022, the average concentration increased from 320.40 ppb to 333.99 ppb, increasing by approximately 0.97 ppb annually. In 2022, the annual average concentration of N_2O at Zhongshan Station increased by 0.68 ppb compared to that in 2021, representing a relative increase of 0.20%.

From 1997 to 2022, all four Antarctic stations monitoring SF_6 showed a significant increasing trend in annual average concentrations (Figure 3.3b). The annual average concentration increased from 3.83 ppt in 1997 to 10.78 ppt in 2022, an increase of approximately 2.8 times. The annual growth rate also showed an increasing trend, from 0.19 ppt/year to 0.38 ppt/year, with an average growth rate of approximately 0.28 ppt/year. In 2022, the annual average concentration of SF_6 at the four Antarctic stations was 10.78 ppt, an increase of 0.38 ppt from 2021, marking the greatest annual increase on record.

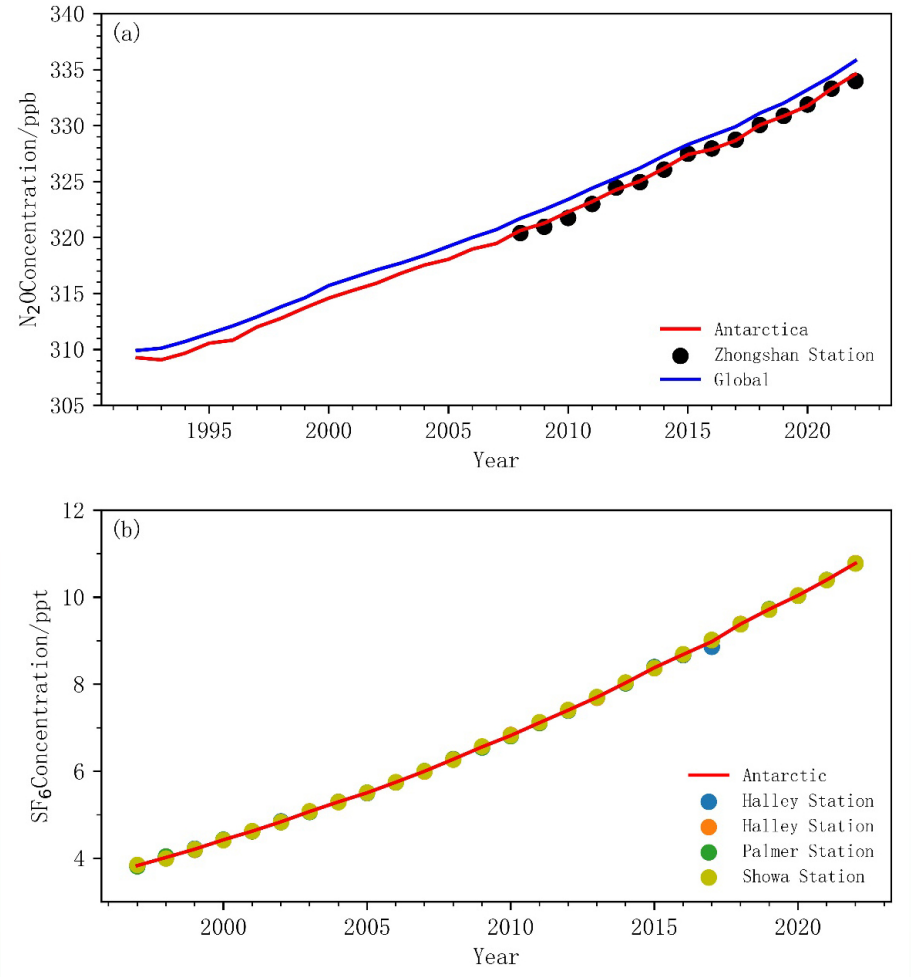

Figure 3.3 Average concentrations of N2O (a, 1992–2022) and SF6 (b, 1997–2022) in Antarctica

3.1.2 Arctic

(1) CO_2 and CH_4

From 1984 to 2022, the concentration of CO_2 in the Arctic atmosphere steadily increased annually (Figure 3.4a), with a growth rate of 1.94 ppm/year. This trend was consistent with the global trend, but the annual average concentration was slightly higher than the global average by 1.78 ppm. In 2022, the annual average concentration of CO_2 in the Arctic atmosphere reached 420.12 ppm, an increase of 2.36 ppm compared to that in 2021. In 2022, the annual average concentration of CO_2 in Waliguan Station, China reached 419.3±0.2ppm,a little bit higher than the global average.

Similarly, from 1984 to 2022, the concentration of CH_4 in the Arctic atmosphere also steadily increased each year (Figure 3.4b), with a growth rate of 5.35 ppb/year. This trend was consistent with the global trend, but the annual average concentration was higher than the global average by 78.36 ppb. In 2022, the annual average concentration of CH_4 in the Arctic atmosphere reached 2004.02 ppb, an increase of 15.66 ppb compared to that in 2021.

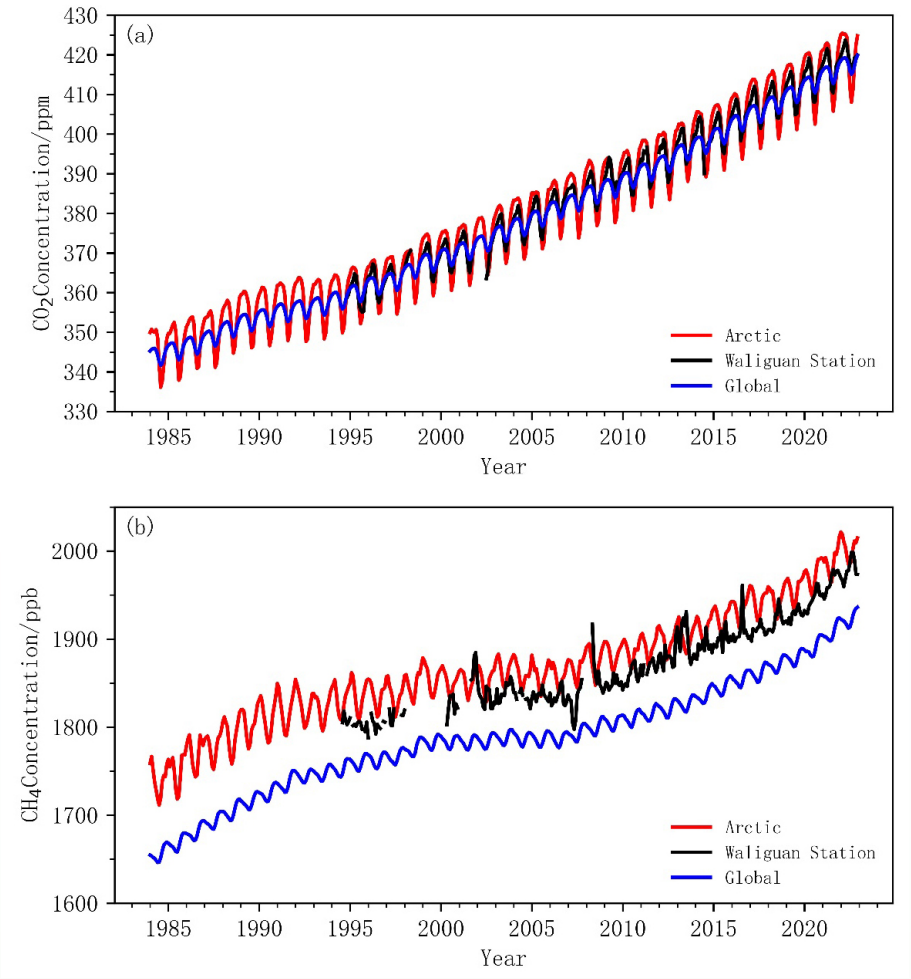

Figure 3.4 Changes in concentrations of CO2 (a) and CH4 (b) in in the Arctic and the globe, 1984 to 2022

(2) N_2O and SF_6

Currently, N_2O is monitored at eight global atmospheric background stations in the Arctic. The average concentration of N_2O at these stations increased from 313.31 ppb in 1997 to 336.08 ppb in 2022, with annual growth rates ranging from 0.43 ppb/year to 1.40 ppb/year and an average growth rate of approximately 0.88 ppb/year (Figure 3.5a). In 2022, the annual average concentration of N_2O in the Arctic increased by 1.34 ppb compared to that in 2021. In 2022, the annual average concentration of CH_4 in Waliguan Station, China reached 1979±0.6ppb.

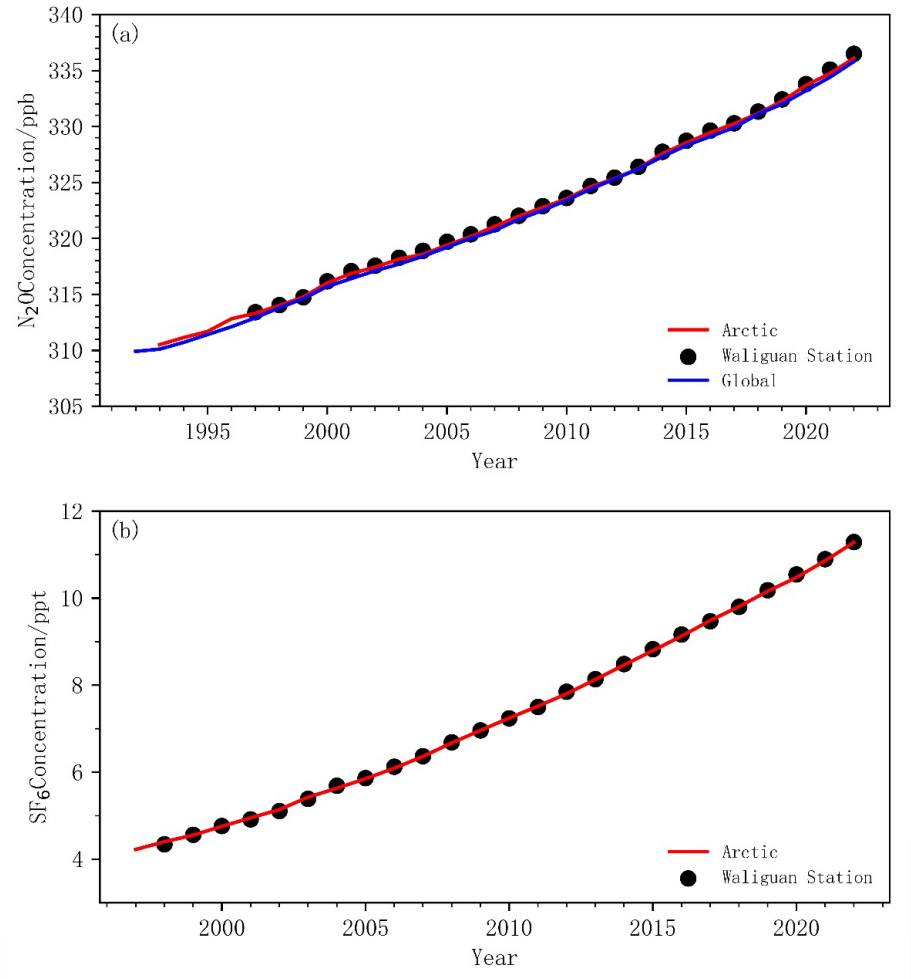

Figure 3.5 Average Concentrations of N_2O (a, 1992–2022) and SF_6 (b, 1997–2022) in the Arctic

The seven Arctic stations monitoring SF_6 showed an increase in average concentration from 4.22 ppt in 1997 to 11.28 ppt in 2022, a nearly 2.6-fold increase. The annual increase also showed an increasing trend, from 0.15 ppt/year to 0.38 ppt/year, with an average growth rate of approximately 0.28 ppt/year (Figure 3.5b). In 2022, the annual average concentration of SF_6 in the Arctic was 11.28 ppt, an increase of 0.42 ppt from 2021, marking the greatest annual increase on record. In 2022, the annual average concentration of SF_6 in Waliguan Station, China was 11.24±0.03ppt.

3.2 Total Ozone in Polar Regions

3.2.1 Antarctic Ozone Hole

In 2023, the ozone hole formed one to two weeks earlier than usual and lasted longer. It began to appear in mid-August, grew to its largest size by mid-September, and reached its peak area on September 21, covering more than 2.6×10^7 km^2. Starting in October, the ozone hole began to shrink and was close to the average size for a period. However, it expanded again toward the end of the month. By early December, it had decreased significantly in size, and it closed on December 20.

Despite significant advancements by the international community in reducing ozone-depleting substance (ODSs) emissions through the Montreal Protocol and related measures, the unusual behavior of the ozone layer over the Southern Hemisphere has attracted the world's attention for four years. From the perspective of short-term factors, some scholars speculate that the eruption of the Hunga-Tonga volcano last year increased stratospheric water vapor, which might lead to the formation of more polar stratospheric clouds and further accelerate ozone depletion. From the perspective of long-term factors, the ban in 1987 slowed down the emissions of ODSs. However, the previously emitted ODSs still remain in the atmosphere and may have an impact for decades. Moreover, by reducing the mixing of atmospheric layers to cooler stratospheric temperatures, global warming might have also contributed to the formation of large and lasting ozone holes in recent years.

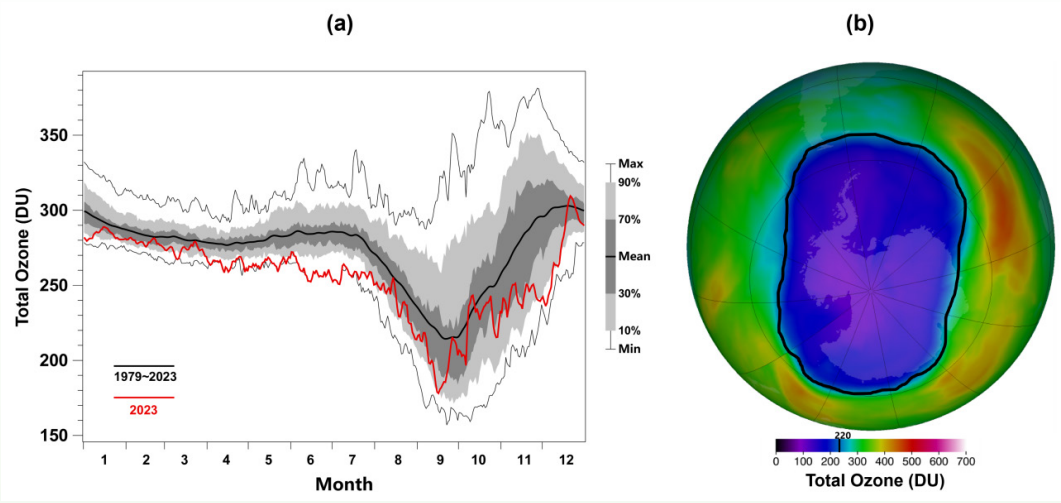

Figure 3.6 (a) Comparison of the change in Antarctic ozone hole area in 2023 with the historical average since 1979. (b) Spatial distribution of the Antarctic ozone hole on September 21, 2023.The black line is the 220DU contour line.

3.2.2 Arctic Ozone Depletion

From the winter of 2023 to the spring of 2024, the total ozone levels not only significantly surpassed the historical average but also quickly increased after a short decrease in February 2024. By mid-March, the ozone levels reached nearly 490 DU (Dobson Units), approaching a record high. In March, the average ozone level over the Arctic was 440 DU, placing it ninth in historical rankings. With warmer stratospheric temperatures over the Arctic in spring, the average temperature at 50 hPa in March was 221 K, making it the sixth highest in historical records. This relatively warm temperature within the polar vortex unfavorable to the formation of polar stratospheric clouds, thus reducing the chances of large-scale ozone depletion this year. The pattern of ozone levels over the Arctic in 2024 followed a trend similar to that in 2023.

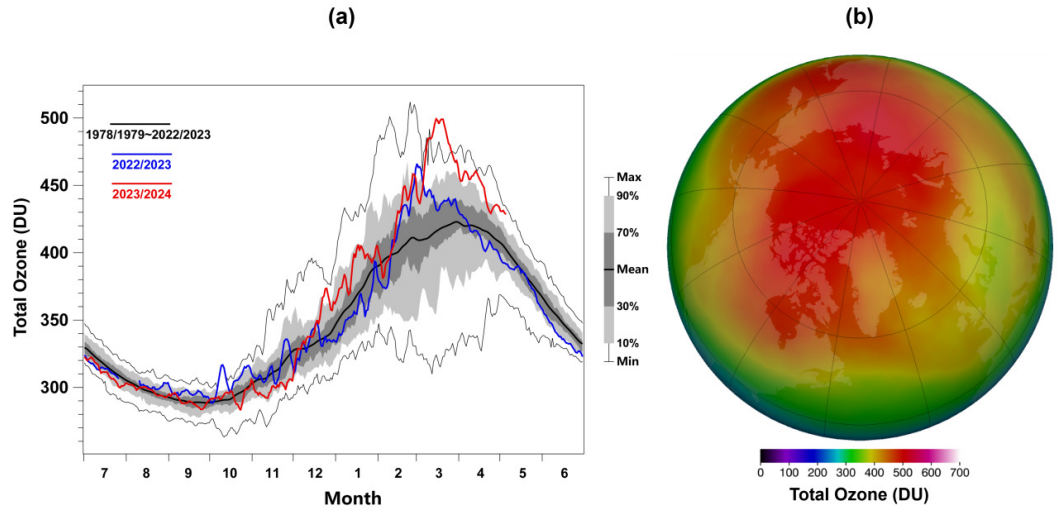

Figure 3.7 (a) Comparison of the average total ozone north of 63°N with the historical average since 1979; (b) Spatial distribution of Arctic total ozone in March 2023

Main Data Sources

1. National Arctic and Antarctic data center(NAADC) Meteorological observation products
   https://datacenter.chinare.org.cn/data-center/dindex
2. China Meteorological Administration Global Atmospheric/Land Surface Reanalysis data (CRA-40)
   http://idata.cma/idata/web/fact/toTechReport2
3. Global Historical Climatology Network - Daily (GHCN-Daily)
   https://www.ncdc.noaa.gov/cdo-web/datasets
4. Global Surface Summary of the Day
   https://registry.opendata.aws/noaa-gsod
5. The British Antarctic Survey
   https://www.bas.ac.uk/project/reader/#data
6. Danish Meteorological Institute
   http://research.dmi.dk/data/
7. National Snow and Ice Data Center
   https://nsidc.org/data/nsidc-0051/versions/2
8. National Satellite Meteorological Center-FENGYUN Satellite Data
   http://data.nsmc.org.cn/portalsite/default.aspx
9. The Earth Science Data Systems of NASA (National Aeronautics and Space Administration)
   https://www.earthdata.nasa.gov/
10. Ocean University of China (OUC)
    http://coas.ouc.edu.cn/pogoc/sjgx/list.htm 11
11. The World Data Centre for Greenhouse Gases (WDCGG)
    https://gaw.kishou.go.jp/publications/global_mean_mole_fractions#content1
12. Goddard Space Flight Center of NASA (National Aeronautics and Space Administration)
    https://ozonewatch.gsfc.nasa.gov/

Glossary

Antarctica: The vast region south of latitude 65°S.

Arctic: The vast region north of latitude 65°N.

Anomaly: The difference between a variable and its multi-year average value for the period 1991 to 2020.

Reanalysis Data: Historical weather data obtained by assimilating model forecasts and observational data through advanced, fixed assimilation systems and numerical forecast models to produce a rich dataset with complete spatial coverage and consistent time series. In this report, reanalysis data specifically refers to the first-generation global atmospheric reanalysis dataset, CRA-40, released by the National Meteorological Information Center.

Antarctic Oscillation(AAO): The seesaw change phenomenon of the pressure field between the Antarctic and the mid-latitudes of the Southern Hemisphere, also known as the Southern Annular Mode(SAM). The AAO Index is defined as the difference between the zonal averages of sea level pressure in two representative latitude zones, 40°S and 70°S, and the SLP data comes from CRA-40 reanalysis dataset.

Arctic Oscillation(AO): The seesaw change phenomenon of the air pressure field between the Arctic and the mid-latitudes of the Northern Hemisphere, also known as the Northern Annular Mode(NAM). The AO Index is defined as the difference between the zonal averages of sea level pressure in two representative latitude zones, 35°N and 65°N, and the SLP data comes from CRA-40 reanalysis dataset.

Polar Vortex: a large-scale low-pressure vortex phenomenon in the polar troposphere and stratosphere, which has an important impact on the climate of the polar regions and mid-high latitudes of the northern and southern hemispheres.

Arctic Polar Vortex Index: An indicator established by Beijing Climate Center and commonly used in climate monitoring services. The area index is defined as the area enclosed by the characteristic contour line of the southern boundary of the polar vortex north of the 500hPa height field in the 0°-360° region of the Northern Hemisphere. The intensity index is defined as the total mass of air between the 500hPa isobaric surface and the contour surface where the characteristic contour line of the southern boundary of the polar vortex is located in the 0°-360° region of the northern hemisphere.

Sea ice concentration: a measurement of the amount of sea ice in a given area, usually described as a percentage.

Sea ice extent: the total region with at least 15 percent sea ice concentration.

Melt Onset(MO): Free water is continuously present with in the snow pack and the ice surface becomes damp at the snow ice interface.

Freeze Onset(FO): The ice is generally bare to lightly snow covered, well drained and the surface layer

of the ice is refrozen.

Greenhouse gases: Natural or anthropogenic gas components in the atmosphere that can absorb and emit longwave radiation from the Earth's surface, atmosphere, and clouds, leading to the greenhouse effect. The major greenhouse gases in the Earth's atmosphere include carbon dioxide (CO_2), methane (CH_4), nitrous oxide (N_2O), sulfur hexafluoride (SF_6), hydrofluorocarbons (HFCs), and perfluorocarbons (PFCs), as specified in the Kyoto Protocol.

PPM: The number of molecules of a given gas per million (10^6) molecules of dry air.

PPB: The number of molecules of a given gas per billion (10^9) molecules of dry air.

PPT: The number of molecules of a given gas per trillion (10^{12}) molecules of dry air.

Greenhouse Gases observation stations in Arctic: Kotelny Island Station (Russia, KOT), Tiksi Station (Russia, TIK), Alert Station (Canada, ALT), Mould Bay Station (Canada, MBC), Barrow Station (USA, BRW), Behchokǫ̀ Station (Canada, BCK), Cambridge Bay Station (Canada, CBY), Inuvik Station (Canada, INU), Zeppelin Mountain Station (Norway, ZEP), Summit Station (Denmark, SUM), Teriberka Station (Russia, TER), Pallas Station (Finland, PAL), Storhofdi Station (Iceland, ICE), Lerwick Station (UK, SIS), Ocean Station Charlie (USA, STC)

Greenhouse Gases observation stations in Antarctica: King Sejong Station (South Korea, KSG), Jubany Station (Argentina, JBN), Palmer Station (USA, PSA), Casey Station (Australia, CYA), Mawson Station (Australia, MAA), Showa Station (Japan, SYO), Halley Station (UK, HBA), Arrival Heights Station (New Zealand, ARH), McMurdo Station (USA, MCM), South Pole Station (USA, SPO), Zhongshan Station (China, ZOS).

Dobson unit (DU): A unit to measure the total amount of ozone in a vertical column above the Earth's surface (total column ozone). The number of Dobson Units is the thickness in units of 10-5 m that the ozone column would occupy if compressed into a layer of uniform density at a pressure of 1013 hPa and a temperature of 0°C. One DU corresponds to a column of ozone containing 2.69×10^{20} molecules per square metre. A typical value for the amount of ozone in a column of the Earth's atmosphere, although very variable, is 300 DU.

Ozone-depleting substances (ODSs): Ozone-depleting substances (ODSs) are man-made gases that destroy ozone (O_3) once they reach the ozone layer in the stratosphere. Ozone depleting substances include: chlorofluorocarbons (CFCs), hydrochlorofluorocarbons (HCFCs), hydrobromofluorocarbons (HBFCs), halons, methyl bromide, carbon tetrachloride and methyl chloroform.

Ozone layer: The ozone layer is a layer of Earth's stratosphere that absorbs most of the Sun's ultraviolet radiation. It contains high concentrations of ozone (O_3) in relation to other parts of the atmosphere, although still small in relation to other gases in the stratosphere.The ozone layer is mainly found in the lower portion of the stratosphere, from approximately 12 to 40 kilometres above Earth, and reach the maxima from 20 to 25 kilometres. Every year, during the spring of the Southern Hemisphere, the ozone layer over the Antarctic region experiences very strong depletion, caused by anthropogenic chlorides and bromides in combination with the region's specific meteorological conditions. This phenomenon is known as the ozone hole.

STATE OF POLAR CLIMATE
2023